RADIOLOGIC AND PATHOLOGIC ANALYSIS OF SOLITARY BONE LESIONS

Part I: Internal Margins

JOHN E. MADEWELL, M.D.

Chairman and Registrar, Department of Radiologic Pathology, Armed Forces Institute of Pathology, Washington, D.C.; Professor of Radiology and Nuclear Medicine, Uniformed Services University of the Health Sciences, Bethesda, Maryland

BRUCE D. RAGSDALE, M.D.

Staff Pathologist, Department of Orthopedic Pathology, Armed Forces Institute of Pathology, Washington, D.C.; Clinical Assistant Professor of Pathology, Uniformed Services University of the Health Sciences, Bethesda, Maryland

DONALD E. SWEET, M.D.

Chairman and Registrar, Department of Orthopedic Pathology, Armed Forces Institute of Pathology, Washington, D.C.; Clinical Associate Professor of Pathology, Uniformed Services University of the Health Sciences, Bethesda, Maryland

Bone lesions have fascinated medical observers since antiquity and have been the subject of much study and controversy. Early in this century, Codman recognized the rarity of bone tumors and hence, the difficulty of accumulating a sufficiently large experience and follow-up to determine efficacy of treatment. His response was the registry concept of tumor study.[8] A clarification of existing nomenclature[6] and a description of new entities, such as the epiphyseal chondromatous giant cell tumor ("Codman tumor")[5] and the reticulum cell sarcoma of bone,[27] evolved from his Registry of Bone Sarcoma. Radiographic features that aid in distinguishing benign from malignant lesions were delineated[6, 7] and it was learned that giant cell tumors are usually not malignant.[6, 9] Further study of the Registry material, augmented by the cases collected at the Armed Forces Institute of Pathology by Doctors L. C. Johnson, G. S. Lodwick, E. G. Theros, and W. L. Thompson, has refined and expanded these contributions. The site frequency (Figs. 1 and 2), peak age of incidence, and numerical frequency of bone tumors indicate that they are not completely autonomous, but are subject to the laws of field behavior and developmental anatomy of normal bone from which they cannot wholely escape and which they may caricature.[15]

The plain radiograph delineates the lesion's location (one or several bones), the segment of involvement (epiphysis, metaphysis, or diaphysis) (Fig. 1), growth characteristics (margins, periosteal reactions) (Table 1), and the presence or absence of calcified tumor matrix which may predict histologic composition.

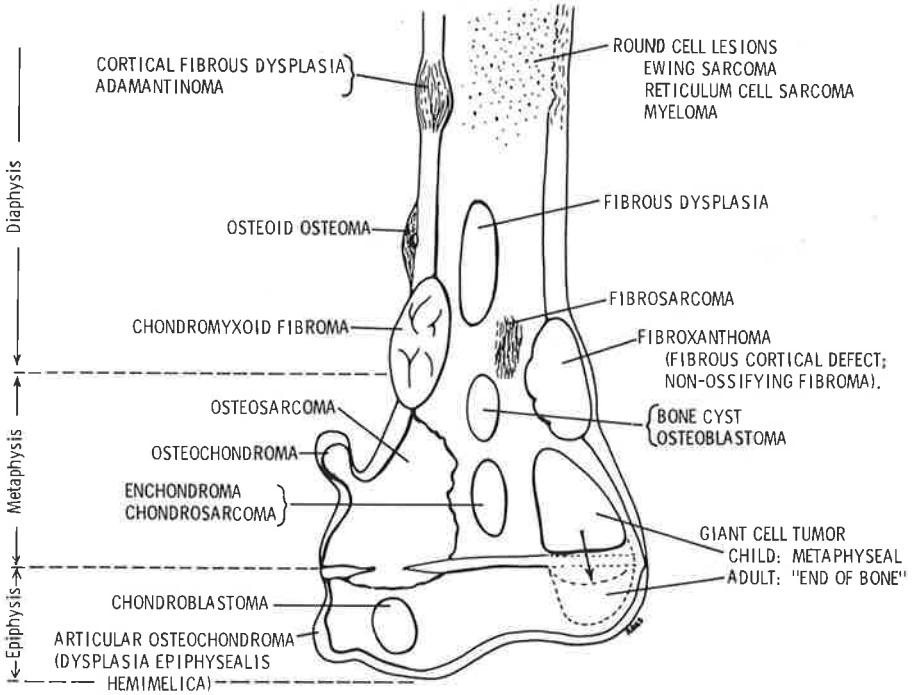

Figure 1. Composite diagram illustrating frequent sites of bone tumors. The diagram depicts the end of a long bone which has been divided into the epiphysis, metaphysis, and diaphysis. The typical sites of common primary bone tumors are labeled. Bone tumors tend to predominate in those ends of long bones which undergo the greatest growth and remodeling, and hence, have the greatest number of cells and amount of cell activity (shoulder and knee regions). When small tumors, presumably detected early, are analyzed, preferential sites of tumor origin become apparent within each bone, as shown in this illustration. This suggests a relationship between the type of tumor and the anatomic site affected. In general, a tumor of a given cell type arises in the field where the homologous normal cells are most active. These regional variations suggest that the composition of the tumor is affected or may be determined by the metabolic field in which it arises.[15]

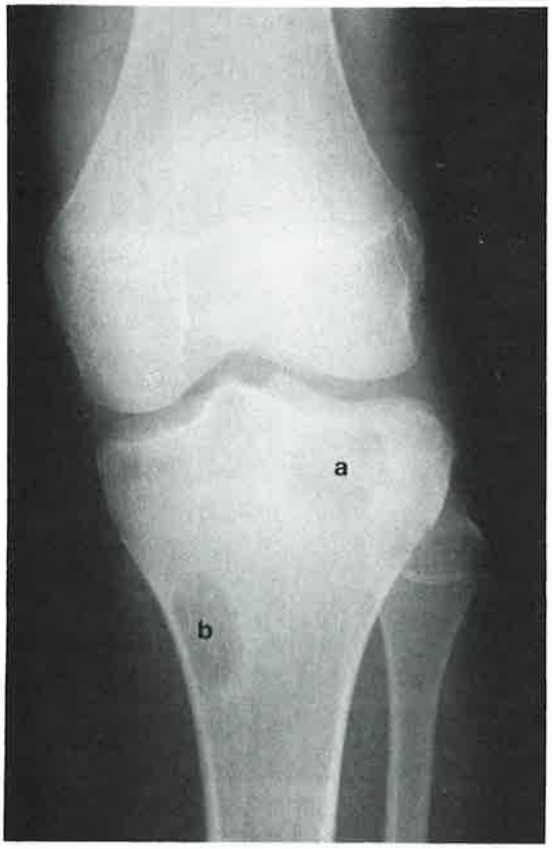

Figure 2. Two lytic lesions, a chondroblastoma *(a)* and a fibroxanthoma or nonossifying fibroma *(b),* are seen. Each lesion has a sharp geographic margin and no periosteal reaction or matrix calcification. Both lesions have similar radiographic patterns, but one is located within the epiphysis (chondroblastoma) and the other in the metadiaphyseal area (fibroxanthoma). This case emphasizes anatomic position as a key factor in predicting diagnosis. (AFIP Neg. No. 68-3263-1.)

Special imaging techniques (bone scanning, angiography, and computed tomography) contribute to the determination of the extent of the disease, and are extremely valuable in planning management. Only rarely do they modify the diagnosis proposed on plain radiographs.

Radiologic information, since it reflects gross anatomy and pathology, must be taken into account during pathologic diagnosis and clinical management. This is not a new concept, as indicated by the following quotation: "The gross anatomy (as revealed in radiographs) is often a safer guide to a correct clinical conception of the disease than the variable and uncertain structure of a small piece of tissue."[12]

CHARACTERISTICS OF NORMAL BONE

Because disease effects its changes by employing and often accentuating normal mechanisms, a knowledge of normal bone biology provides a key to analysis of alterations evoked by bone tumors. Against this background, a brief review is in order.

The term bone refers both to a tissue and to an organ. Whether inspected directly or by radiographic technique, a normal bone (organ) is constructed of two types of bone (tissue): cancellous bone (spongy or trabecular), or cortical bone (compact).

Cancellous Bone

Cancellous bone is the lattice of interconnected bony spicules that compartmentalize the marrow space. It comprises the bulk of the square bones (for example, the calcaneus), but in long tubular bones, is mainly confined to the epiphysis and metaphysis. Only a small amount of cancellous bone is present in the diaphysis along the inner surface of the cortex. In long bones, the primary function of cancellous bone is to support the subarticular bony endplate and to transmit mechanical force from the articular surface to the cortex.

The amount and architectural orientation of cancellous bone are largely determined by the changing force on each bone.[16, 32, 33] This can be illustrated by observing the change in trabecular pattern of the proximal femur before and after closure of the growth plate (Fig. 3). The force-diffusing characteristic of

TABLE 1. *Relationship of Biologic Activity (Growth Rate) to Type of Margin and Periosteal Reaction*

GROWTH RATE	INTERNAL MARGINS	PERIOSTEAL REACTION
Slow	Geographic (I) IA IB IC	Solid
Intermediate	Moth-eaten (II)	Shells Ridged Lobulated Smooth
Fast	Permeative (III)	Lamellated
Fastest	Nonvisible	Spiculated or none

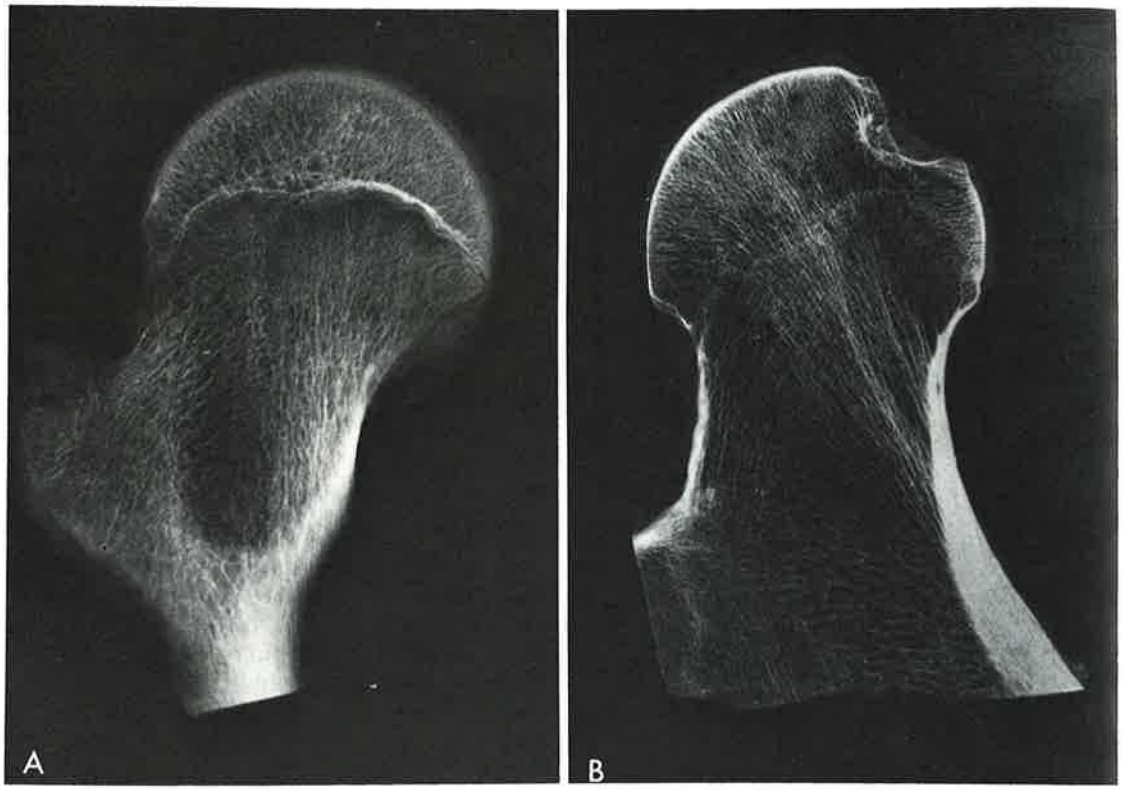

Figure 3. Normal femoral heads. Specimen radiographs of the femoral head and neck with a closing femoral epiphysis *(A)* and with a closed growth plate *(B)*. Note the differing amounts and orientation of cancellous bone, especially in the epiphysis of each patient. This reflects the changing mechanical requirements as the growth plate closes. (AFIP Neg. Nos. 79-6007, 79-6008.)

the epiphyseal growth plate cartilage that is interposed, in growing bone, between the articular surface and the cortical shaft results in a tightly packed, crossing pattern of cancellous bone throughout the epiphysis (Fig. 3*A*). This pattern is independent of the trajectorial arrangement of cancellous bone in the metaphysis. Under these circumstances, metaphyseal cancellous bone supports the growth plate, and the growth plate, in turn, provides the base of support for epiphyseal cancellous bone supporting the articular surface. Closure of the growth plate is followed by extensive architectural reorganization (remodeling), primarily of the epiphyseal and, to a lesser extent, the metaphyseal cancellous bone, thereby creating an integrated continuum (Fig. 3*B*). The resultant tightly packed thicker cancellous bone trabeculae which support the dominant weight-bearing articular surface represent a direct response to increased mechanical force transmitted through this area. Wolff's law observes that normal bone modifies the mass and orientation of its structural elements to meet functional demands.[33] In diseased bones, similar mechanisms operate to preserve stress-structure relationships as long as possible. The most important mechanical components are retained and are often strengthened, while the more expendible components are lost. This principle, in part, explains the development of a sclerotic margin around slowly growing bone lesions.

Gain and loss of cancellous bone density is traditionally attributed to the "endosteum," a hypothetical, thin, continuous layer of connective tissue that covers the inner surface of the cortex and envelops each trabecula. Such a layer is not a usual feature of mature adult bone, either at the light[29] or electron microscopic level. If the term is to be retained, then its true identity in the resting state as a layer of fatty or hematopoietic marrow should be kept in mind.[4, 24] In the process of skeletal maturation, the mature fat cell replaces the hematopoietic elements as the predominant cell in contact with the endosteal surface of the appendicular skeleton.[29] In disease states, a reactive zone of spindle cells, osteoblasts,

and osteoclasts appears on endosteal surfaces. This is the earliest stage of regional fibrovascular marrow transformation, a stereotyped, nonspecific reaction of bone marrow to various stimuli. It is also the initial step toward osteoclasia and osteosclerosis. The most likely source for this reactive fibrovascular marrow is modulation of antecedent normal marrow.

Cortical Bone

Cortical bone is most concentrated in the diaphysis, thinning gradually toward the end of the bone where cancellous bone increases and assumes the weight-bearing function. Thus the concentration of cortical bone is minimal wherever the concentration of cancellous bone is greatest, and vice versa. Mature cortical bone is composed of multiple, longitudinally oriented cylinders of bone with one or more central vessels. Each cylindrical unit is termed a haversian system or osteone.[10, 16, 17] The central or haversian canals of the various osteones are interconnected by perpendicular vascular passages called Volkmann's canals. Remodeling of cortical bone entails osteone formation. This begins with longitudinally oriented tubular resorption cavities formed by "cutting cones" of cooperative osteoclasts (Fig. 20, *C* and *D*). The tubular holes are subsequently refilled by concentric layers of lamellar bone. Removal and refill are normally simultaneous and balanced with no change in cortical density until older age. If resorption exceeds refill, there is less cortical bone; this appears radiographically as a "tunneled cortex" giving rise to a permeative osteolytic pattern.[13, 16, 17, 25, 26, 31]

Effect of Bone Lesions

Lytic and blastic alterations associated with bone lesions are mediated by osteoclasts and osteoblasts, respectively, and result in interfaces or margins. Bone destruction associated with neoplasia is not a direct effect of tumor cells but is accomplished by normal host osteoclasts in response to pressure generated by the enlarging mass or its associated active hyperemia. This fact is often obscured by expressions such as "tumor destruction." A possible exception is giant cell tumor, a tumor composed of osteoclasts (osteoclastoma), but even this is contested.[30]

The lysis seen in radiographs is the summation of osteoclastic resorptive activity on cortical and trabecular bone surfaces. This activity is twofold: removal of the mineral component of bone matrix,[14] followed by enzymatic digestion[3] and possible mechanical abrasion of the collagenous fabric. Resorption always involves the complete removal of a given volume of matrix and because of this fact, the descriptive terms "lytic change," "osteolysis," "osteoporosis," and "osteopenia" are preferred to "demineralization."

Individually, osteoclasts can destroy bone much faster than osteoblasts can produce it.[17] Both activities always coexist to some degree. A particularly common microscopic observation is osteoclastic activity on the side of a trabecula against which tumor impinges, and osteoblastic activity on the opposite side. The relative predominance of one over the other will eventually be evident as a visible margin in the radiograph.

This article and the two that follow it will attempt to define and illustrate three radiologic aspects of tumors: margins (Part I), periosteal reactions (Part II), and matrix production (Part III). This will be accomplished through radiologic-pathologic correlation utilizing the case example technique used by Phemister.[28] Other entities often associated with similar radiographic features are mentioned, but an exhaustive differential diagnosis is not tabulated for each pattern. The value of large histologic sections in understanding radiologic patterns will be emphasized.

MARGINS

The perception of osteolysis on plain radiographs depends on the structure of bone (cancellous versus cortical), the degree of bone loss,[1, 2, 18] and the amount of adjacent host bone available for contrast.[19, 21] Space-occupying processes will be more apparent toward the end of a bone where the quantity of cancellous bone is greater, providing increased contrast. A benign, lucent, space-occupying lesion formed in the metaphysis can be seen because of adjacent intact trabeculae. It may later be "lost" on radiographic examination as normal growth and remodeling remove surrounding cancellous bone and the host metaphysis becomes diaphysis. This phenomenon may explain the instance of "spontaneous disappearence" as may occur in fibroxanthomas.

Figure 4. Enchondroma of the fifth metacarpal bone with fracture. The focal lytic lesion has a scalloped edge, widened bone contour, sclerotic rim, and diaphyseal component. The sclerotic rim *(arrow)* is noted only in the cancellous portion of bone. The diaphyseal component has no sclerotic rim but is seen because of the endosteal scalloping and fusiform widening of the marrow space. Sclerotic rims are uncommon in the diaphysis because there is little or no cancellous bone. When a lesion impinges on both cancellous (metaphysis) and compact (diaphysis) bone, an indistinct or invisible diaphyseal margin by itself, does not necessarily indicate that the tumor is growing more rapidly in the diaphyseal area. Rather, it means that there is no trabecular bone upon which a sclerotic rim can form. (AFIP Neg. No. 335968-1.)

Since there is little cancellous bone in the diaphysis, the limited border modification available to a purely diaphyseal lesion is scalloping of the endosteal surface of the cortex. The ends of the lesion abutting the noncancellous marrow space will not be seen on plain radiographs. Similarly, the full extent of a metaphyseal lesion that extends into the diaphysis may not be evident (Fig. 4).

Cancellous bone, because of its large surface area, is destroyed more rapidly than is cortical bone. Since destruction occurs on small trabecular units throughout the area of lysis, large amounts (30 to 50 per cent) of trabecular bone must be removed before the loss is evident on radiography.[1, 2, 11, 18, 19] Cortical bone destruction occurs at a slower rate but is more easily seen and may be appreciated earlier becuase of the great contrast in density created by focal lysis. The more diffuse cortical change of permeation requires removal of even greater amounts of bone in order to be perceived on radiography. The amount of host bone is particularly important to keep in mind when evaluating elderly patients in whom generalized bone loss occurs. In these patients, destructive lesions are more difficult to detect early, and even advanced infiltrative processes may not be apparent.

The growth of a bone tumor induces normal host osteoclasts and osteoblasts to modify bone structure locally, regionally, and diffusely according to three radiographic patterns (Figs. 5 and 6):

Type I: Geographic pattern — slow

Type II: Moth-eaten pattern — intermediate

Type III: Permeative pattern — rapid

These patterns are an index of growth rates,[19-23] but tell little about the histology of the lesion.[19, 23] Type I predominantly represents an effect on cancellous bone, Type III represents an effect on the cortex, and Type II can result from lysis of either cortical or cancellous bone, or both.

Geographic Bone Destruction (Type I)

This type of destruction creates a well-circumscribed lesion with a narrow zone of transition. Occasionally, its border may be arcuate, lobulated, or scalloped. This pattern implies a slow growth rate that permits time for destruction of all bone in the path of tumor enlargement. It may be slow enough to permit time for accumulation of a reactive bone border (sclerotic rim). The geographic pattern of destruction can be further divided into three subtypes which correlate with rates and manner of growth. Biologic activity increases from IA to IC as follows:

IA: Geographic lesion with sclerosis in the margin

IB: Geographic lesion with no sclerosis in the margin

IC: Geographic lesion with an ill-defined margin

Geographic Lesion with Sclerosis in the Margin (Type IA). This type of lesion most

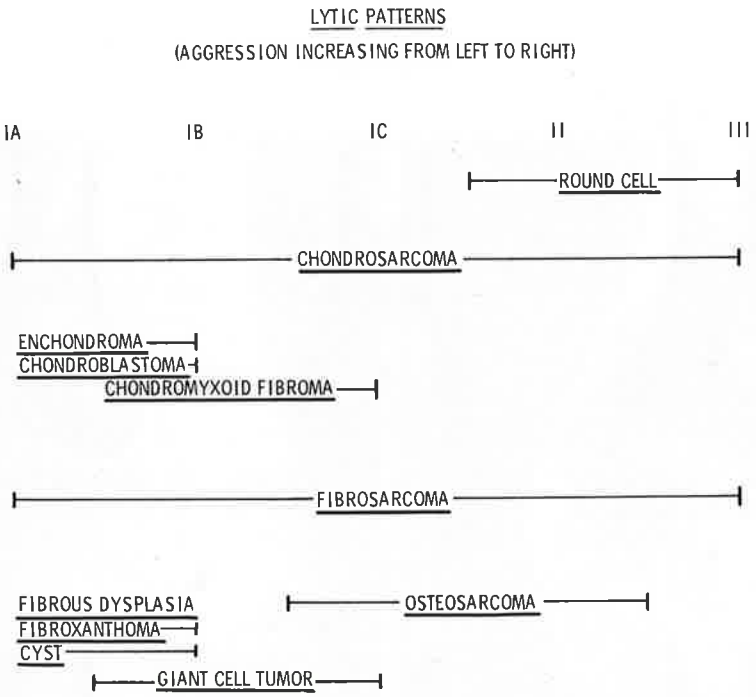

Figure 5. This diagram delineates common bone tumors and their typical patterns of bone destruction. *IA,* Geographic destruction, well-defined, with sclerosis in margin. *IB,* Geographic destruction, well-defined, but no sclerosis in margin. *IC,* Geographic destruction with ill-defined margin. *II,* Moth-eaten (regionally invasive). *III,* Permeative (diffusely invasive). Note that most benign tumors occur on the left-hand side, from IA to IC, whereas most malignant tumors occur on the right-hand side, from IC to III. This illustrates the general principle that the biologic activity and probability of malignancy increase from left to right. Chondrosarcoma and fibrosarcoma can present with any of the five patterns. In our experience, they frequently arise in pre-existing benign lesions. In such cases, the radiographic pattern may lag behind the histologic activity, producing a radiographic discrepancy (slow-appearing lesion with malignant histology).

commonly represents a benign disorder with indolent growth, such as bone cysts (Fig. 8*B*), enchondroma (Fig. 8*C*), fibroxanthoma (Fig. 7), chondromyxoid fibroma (Fig. 8*D*), chondroblastoma, Brodie's abscess, and fibrous dysplasia (Fig. 8*A*). Indolent growth permits development of a reactive rim of bone characteristic of a type IA margin (Fig. 8). The sclerotic rim can vary in thickness and is especially thick when slow-growing lesions occur in weight-bearing or mechanically stressed bones, such as the femur (Fig. 8*B*), tibia, radius, and humerus. The surface of the rim is usually slightly sharper on the outer edge (Fig. 7). Histologically, it is a sheet of lamellar bone extending between truncated antecedent trabeculae about the lesion (Fig. 7*D*). With larger lesions, there may be associated widening of the cortical outline secondary to periosteal activity.

The sclerotic rim is a mechanical adaptation designed to accommodate forces transmitted around the space-occupying mass. Indigenous osseous metaplasia in the benign fibro-osseous tumor group, especially in fibrous dysplasia and fibroxanthoma, may contribute some bone density to the sclerotic rim seen in clinical radiographs (Figs. 7*D* and 8*A*). For the surgeon who is intent upon total removal of a lesion having a sclerotic rim, it is important to know that occasionally, a small portion of tissue from the lesion may extend into and even a short way beyond the radiodense border into the marrow. Microscopic residua are, therefore, possible when portions of the sclerotic rim persist in postoperative radiographs.

Some type IA lesions have a sclerotic rim that fades gradually and imperceptibly into the adjacent cancellous pattern (Fig. 9). A fading sclerotic rim is seen most frequently with chronic osteomyelitis, Brodie's abscess, and occasionally, with eosinophilic granuloma. The fading or "fuzzy" sclerotic zone corresponds pathologically to bone reinforcement (appositional thickening) of surrounding cancellous bone. Frequently, in the marrow space between the thickened trabeculae, a chronic, low-grade, inflammatory response is noted.

Text continued on page 726

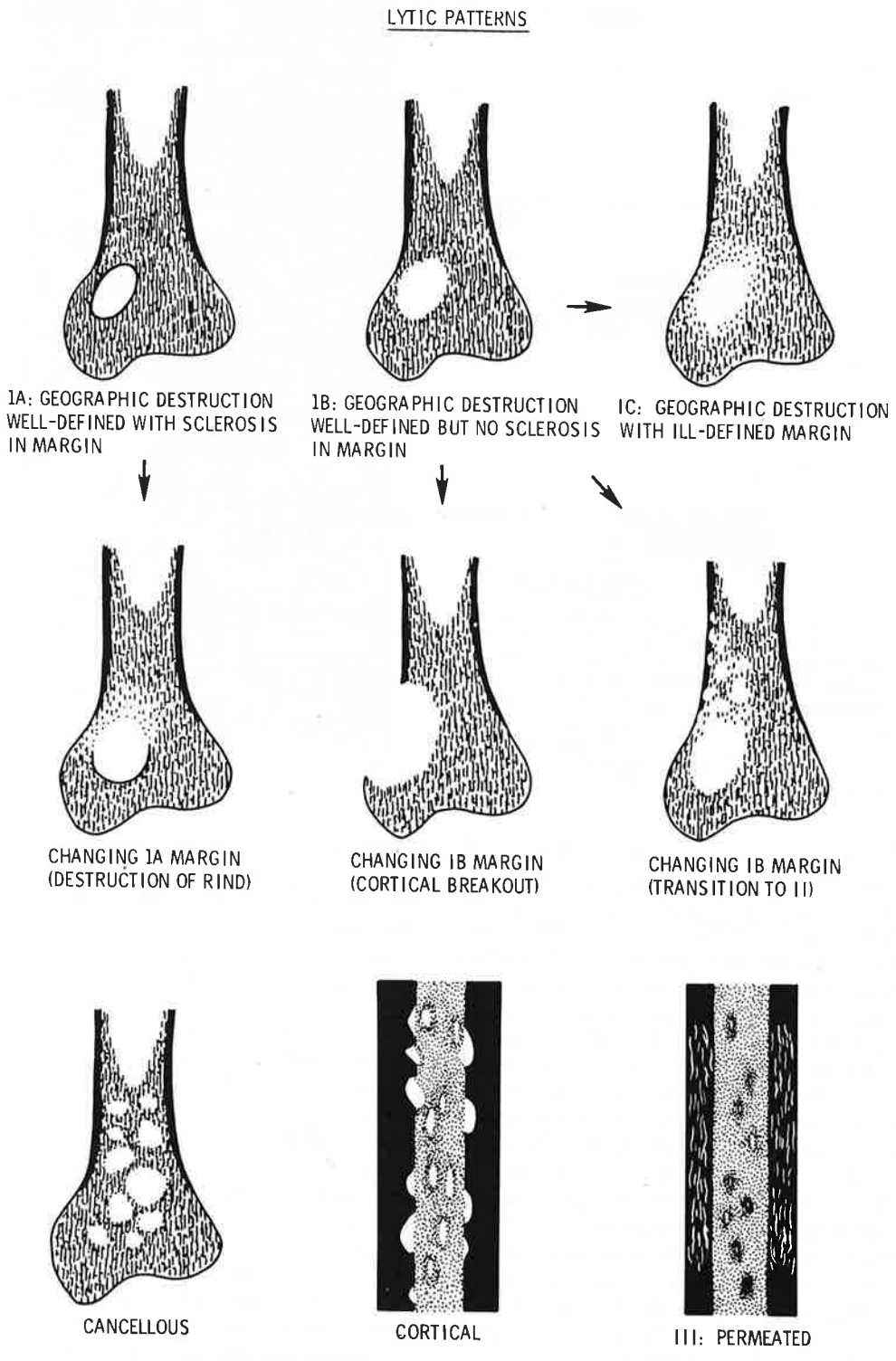

Figure 6. Schematic diagram of patterns of bone destruction (types IA, IB, IC, II, III) and their margins. Arrows indicate the most frequent transitions or combinations of these margins. Transitions imply increased activity and a greater probability of malignancy.

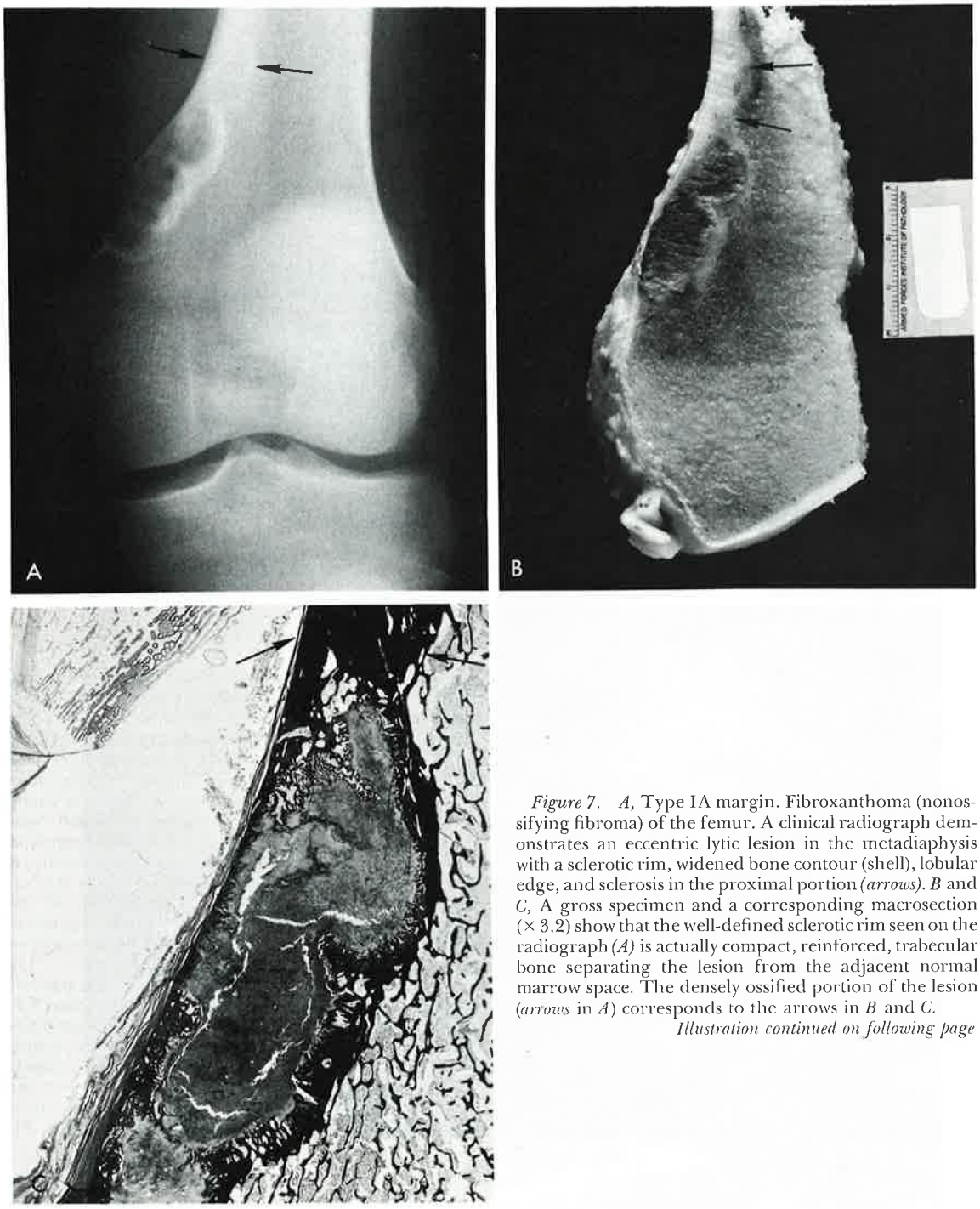

Figure 7. *A,* Type IA margin. Fibroxanthoma (nonossifying fibroma) of the femur. A clinical radiograph demonstrates an eccentric lytic lesion in the metadiaphysis with a sclerotic rim, widened bone contour (shell), lobular edge, and sclerosis in the proximal portion *(arrows). B* and *C,* A gross specimen and a corresponding macrosection (× 3.2) show that the well-defined sclerotic rim seen on the radiograph *(A)* is actually compact, reinforced, trabecular bone separating the lesion from the adjacent normal marrow space. The densely ossified portion of the lesion (*arrows* in *A*) corresponds to the arrows in *B* and *C.*

Illustration continued on following page

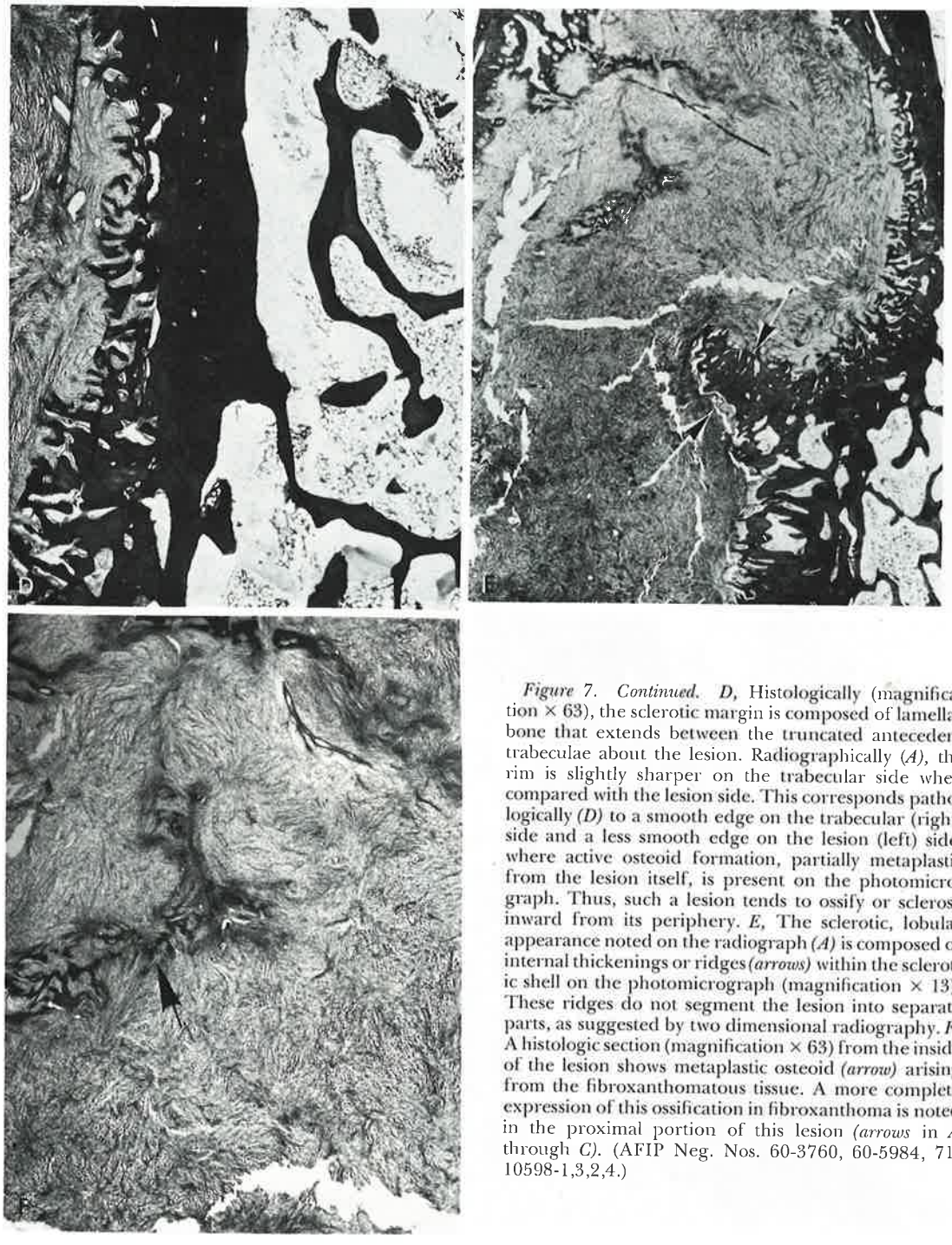

Figure 7. Continued. D, Histologically (magnification × 63), the sclerotic margin is composed of lamellar bone that extends between the truncated antecedent trabeculae about the lesion. Radiographically *(A),* the rim is slightly sharper on the trabecular side when compared with the lesion side. This corresponds pathologically *(D)* to a smooth edge on the trabecular (right) side and a less smooth edge on the lesion (left) side, where active osteoid formation, partially metaplastic from the lesion itself, is present on the photomicrograph. Thus, such a lesion tends to ossify or sclerose inward from its periphery. *E,* The sclerotic, lobular appearance noted on the radiograph *(A)* is composed of internal thickenings or ridges *(arrows)* within the sclerotic shell on the photomicrograph (magnification × 13). These ridges do not segment the lesion into separate parts, as suggested by two dimensional radiography. *F,* A histologic section (magnification × 63) from the inside of the lesion shows metaplastic osteoid *(arrow)* arising from the fibroxanthomatous tissue. A more complete expression of this ossification in fibroxanthoma is noted in the proximal portion of this lesion *(arrows* in *A* through *C).* (AFIP Neg. Nos. 60-3760, 60-5984, 71-10598-1,3,2,4.)

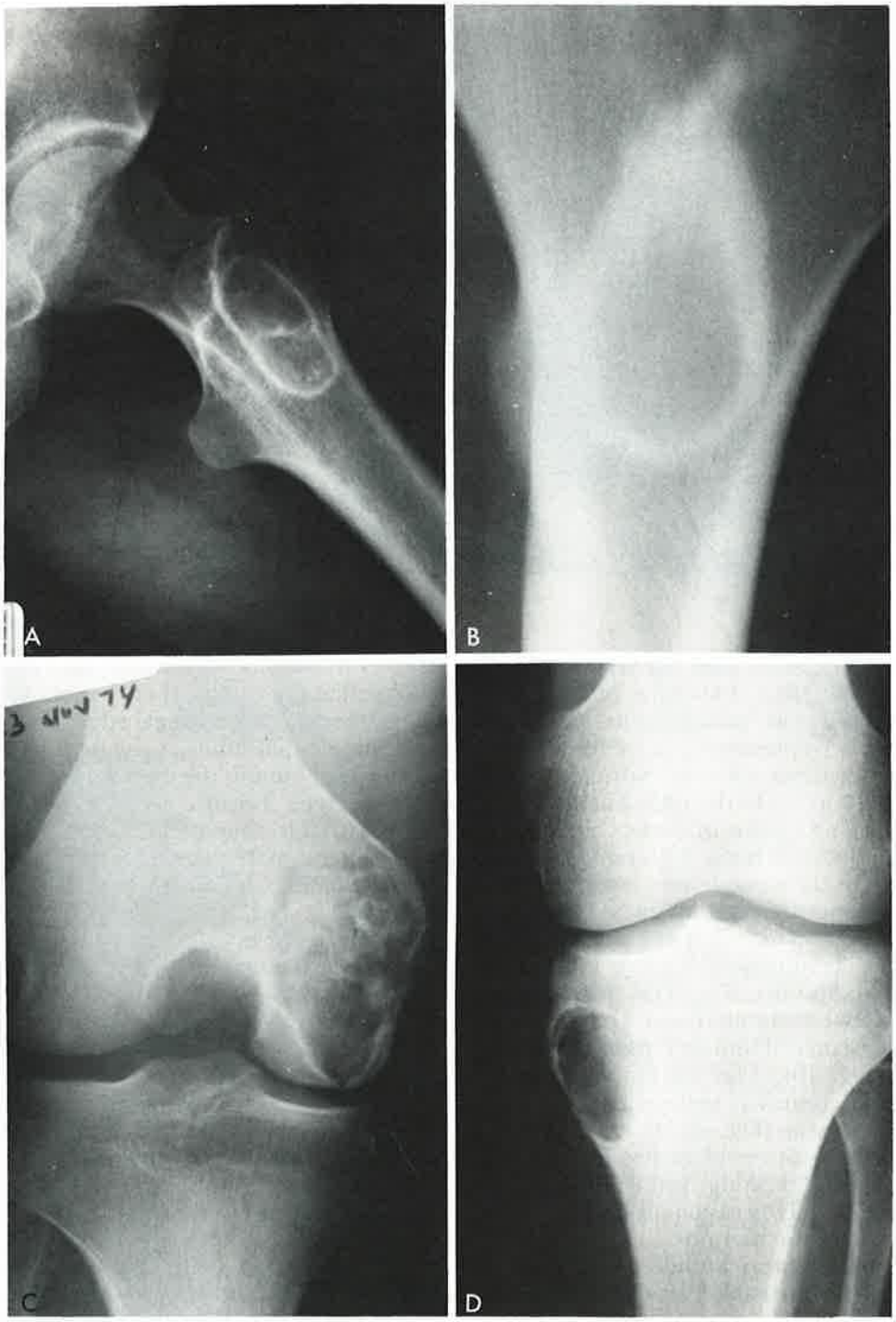

Figure 8. Type IA margins are illustrated in four cases with different diagnoses. *A,* Fibrous dysplasia of the femur. *B,* Bone cyst of the femur. *C,* Enchondroma of the femur. *D,* Chondromyxoid fibroma of the tibia. Each of these lesions has a well-defined sclerotic rim that separates the periphery of the lesion from the adjacent cancellous bone. The dense radiographic margin indicates that these lesions are slow-growing, but is nonspecific for diagnosis. The enchondroma *(C)* has typical arcuate shadows, stippled areas of calcified cartilage matrix, and a lobular margin. These features are highly suggestive of enchondroma. The other lesions are radiographically less specific and their diagnoses are suggested by the anatomic site and clinical history. (AFIP Neg. Nos. 77-1826-1, 72-4158-1, 75-5189-1, 69379-1.)

Figure 9. Type IA margin with fading outer edge. Brodie's abscess of the tibia. This lytic lesion has a very sharp inner edge with a sclerotic rim that fades imperceptibly into the adjacent trabecular bone. This fading sclerotic margin represents trabecular reinforcement over a wide zone about the lesion and a gradual transition to normal trabecular thickness, rather than the sharp transition seen in the more typical IA margins (see Fig. 7). A fading IA margin is commonly associated with inflammatory disease (osteomyelitis, Brodie's abscess, eosinophilic granuloma). (AFIP Neg. Nos. 66-10886-1.)

Geographic Lesion with No Sclerosis in the Margin (Type IB). This type of lesion has been referred to as "punched out" since it has sharp edges (representing a narrow zone of transition) without sclerosis. Normal trabeculae are present up to the edge but are totally removed along a plane of contact between the tumor and normal bone. This sign characterizes many of the same lesions associated with type IA patterns, such as giant cell tumor (Fig. 10), bone cysts (Fig. 11*A*), enchondroma (Fig. 11*D*), chondroblastoma (Fig. 11*C*), chondromyxoid fibroma (Fig. 11*B*), and fibrous dysplasia, but a slightly faster growth rate is involved. Giant cell tumors typically have a IB margin (Fig. 10). The margin seen on the radiograph accurately reflects the true edge of the neoplasm (Fig. 10, *C* and *D*). Since these solid tumors tend to present cohesive extension with "pushing" rather than infiltrative borders, only occasionally will tumor be found beyond the margins.

Diaphyseal tumors limited to the marrow space may be "invisible" on the plain radiograph because there is no cancellous bone to define their edge. They are seen only if they evoke change in the normal density of bone by clastic or blastic activity of the adjacent cortex, by production of a periosteal reaction, or by mineralization of the tumor matrix. As "invisible" intramedullary lesions grow, they frequently erode the inner surface of the cortex by osteoclastic activity, and the resulting scalloping makes them visible (Fig. 12). The interface or endosteal edge, if sharp, has the same implications as the type IB pattern. The edge abutting the marrow space may still not be seen because of lack of bone for contrast; this should not be interpreted as indicating a more aggressive pattern.

Geographic Lesion with Ill-defined Margins (Type IC). This type of geographic lesion is a locally infiltrative process. The tumor extends into the marrow space between trabeculae in advance of the osteolytic edge (Fig. 13*B*). Destruction occurs through a wider zone than is created by the narrow interface that characterizes the IB margin, which is responsible for its ill-defined appearance (Fig. 13, *C* and *D*). It is associated with greater biologic activity than are the IA and IB margins. Lesions typically seen with this pattern include giant cell tumor (Fig. 14*B*), osteosarcoma (Fig. 14*D*), fibrosarcoma (Fig. 13), chondrosarcoma (Fig. 14*C*), active enchondroma (Fig. 14*A*), and chondromyxoid fibroma.

Moth-eaten Destruction (Type II)

This pattern of destruction consists of multiple scattered holes which vary in size, arise separately rather than from the edge of a major central lesion, and then appear to coalesce. Cancellous (Fig. 16) or cortical (Fig.

Text continued on page 733

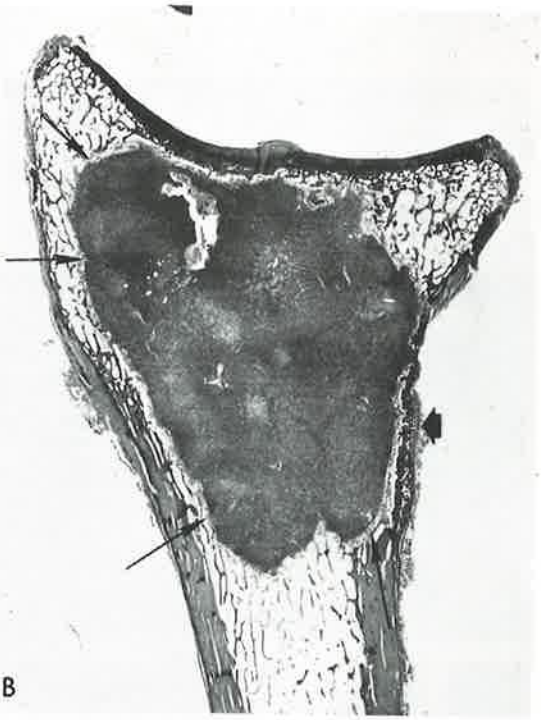

Figure 10. Type IB margin. Giant cell tumor of the radius. *A,* This well-defined, lytic lesion extends to the subarticular bony plate, with widening of the bone contour (shell) on the ulnar side. The lesion extends into the diaphysis where there is cortical destruction *(arrows)* that contributes to the proximal lytic edge. *B,* A macrosection (magnification × 2.3) reveals the solid giant cell tumor with a small cystic component distally. The lesion presents a sharp, cohesive, peripheral surface *(arrows)* to the cancellous bone in the metaphysis and to the cortical bone in the diaphysis. The shell of periosteal new bone production is marked *(arrowhead). C,* A coned-down view of the radiograph displays the interface between the tumor and the cancellous bone. It is a sharp geographic margin with no sclerosis *(arrows)*

Illustration continued on following page

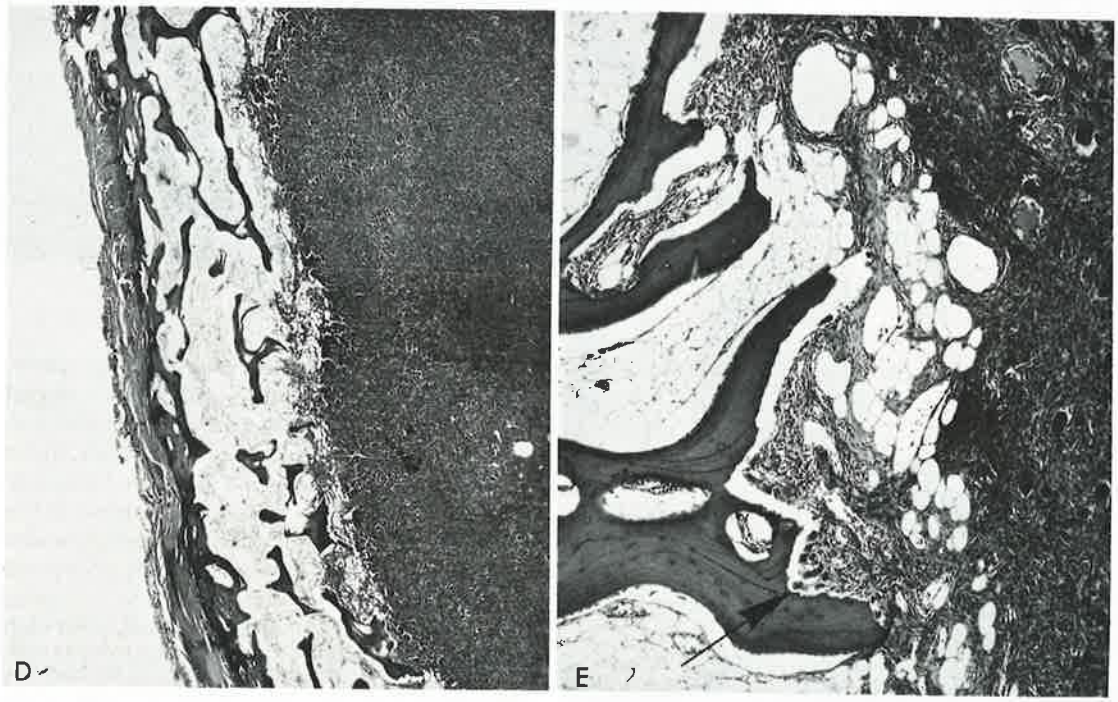

Figure 10 Continued. *D*, Histologically (magnification × 12), the edge is well defined, correlating with the radiograph. The tumor's edge coincides with the lytic margin demonstrated on radiograph. *E*, A photomicrograph (magnification × 63) shows the interface between the tumor (*right*) and trabecular bone (*left*) where surrounding trabeculae are truncated by osteoclastic resorption (*arrow*). These smaller, resorptively active osteoclasts are most likely non-neoplastic components of the activated endosteum which have been induced, by the growth pressure or active hyperemia of the adjacent giant cell tumor, to resorb bone. (AFIP Neg. Nos. 64-4473-1, 70-11536-1, 64-4473-2, 70-11536-1, 64-4473-2, 70-11536-2, 81-13773.)

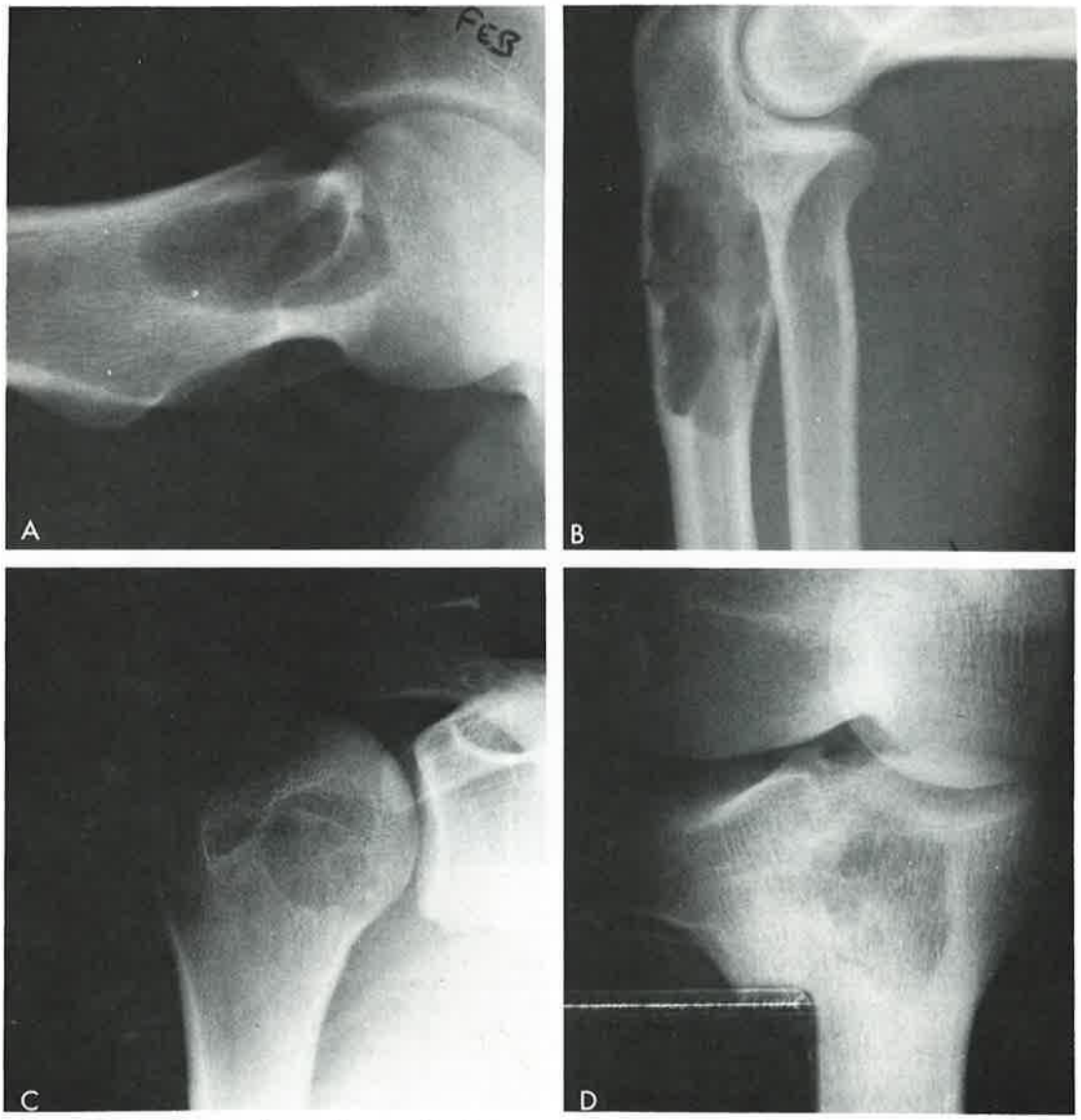

Figure 11. Type IB margins are illustrated in four cases with different diagnoses. *A,* Bone cyst of the femur. *B,* Chondromyxoid fibroma of the ulna. *C,* Chondroblastoma of the humerus. *D,* Enchondroma of the tibia. The chondromyxoid fibroma *(B)* has a diaphyseal component represented by endosteal scallops. The radiograph *(B)* also shows a widened bone contour secondary to periosteal reaction (shell) and a pathologic fracture. (AFIP Neg. Nos. 73-12774-2, 66-3816-1, 71-2420, 76-9552-9.)

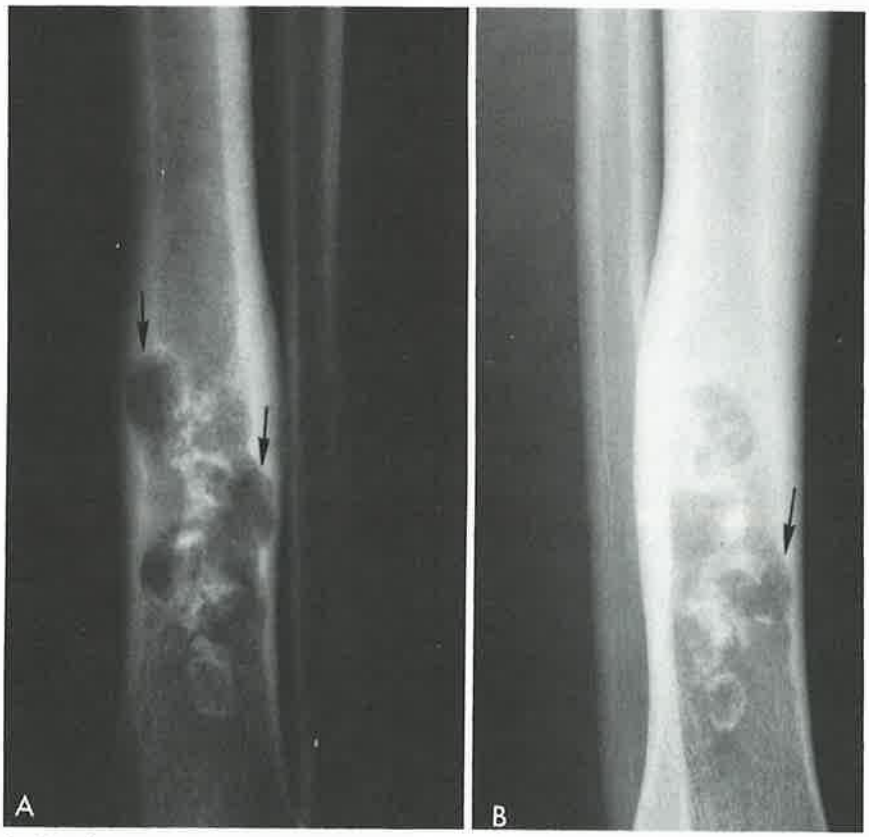

Figure 12. Scalloped pattern. Enchondroma of the tibia. Anteroposterior *(A)* and lateral *(B)* views of the distal tibia show a lytic process, predominantly in the diaphysis, with some involvement of the adjacent metaphysis. Typical stipples, rings, and arcs of mineralization strongly suggest cartilage tumor. Endosteal scalloping *(arrows)* corresponds to the typical lobular growth of cartilage tumors. The consequent focal pressure incites osteoclastic removal of the inner cortex. A solid periosteal reaction widens the bone outline over some of the larger endosteal areas of scalloping. At surgery, the lesion was found to extend several centimeters beyond the most proximal endosteal scallop seen on the radiograph. Radiographically, the only manifestation of this extension is slight endosteal widening. Lesions that displace diaphyseal marrow but fail to evoke endosteal scalloping, produce a calcified matrix, or incite a periosteal reaction will not be seen on the plain radiograph. Mineralization occurs predominantly in the central, older portions of this large, lobular enchondroma. The younger, growing, peripheral, lucent (nonmineralizing) portions of the enchondroma incite the scalloping. (AFIP Neg. Nos. 73-5577-1,2.)

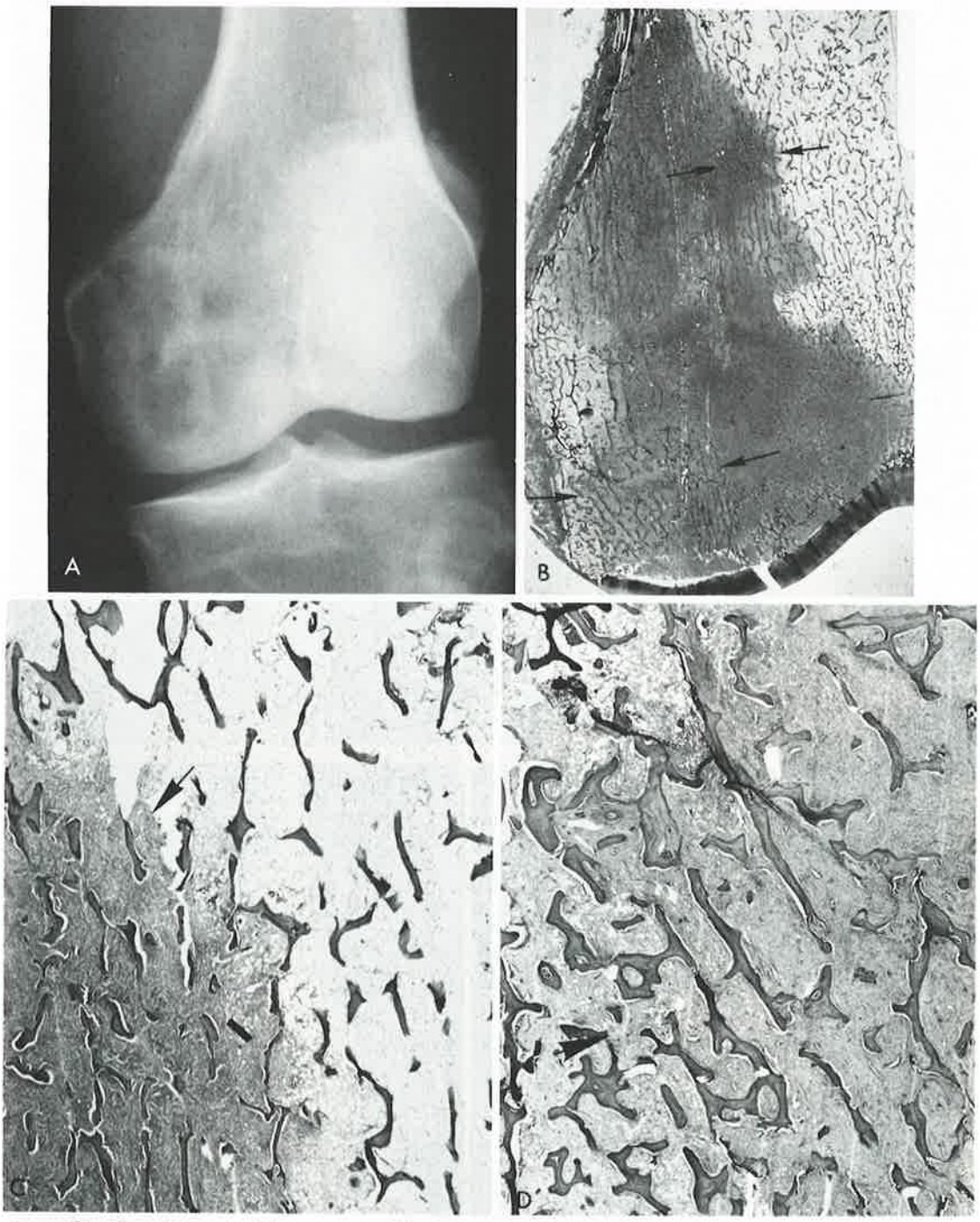

Figure 13. Type IC margin. Fibrosarcoma of the femur. *A,* A clinical radiograph shows a geographic lytic process in the distal femur with cortical destruction laterally and minimal periosteal reaction. The edge of the lesion is ill defined with no sharp margin differentiating the area of bone destruction from the adjacent trabecular bone. This radiographic appearance correlates with local infiltrative growth. *B,* A macrosection (magnification × 1.9) confirms that this geographic lytic process (IC) is attributable to local infiltrating tumor growth within cancellous bone *(arrows).* More centrally, there are patches, with no persisting cancellous bone, that correspond to the central lucent areas of the radiograph. *C* and *D,* Infiltrating growth into the marrow space with partial retention of trabecular bone about the edge is demonstrated on photomicrographs (magnification × 87) taken from the ill-defined margin (*C,* left upper edge, *D,* right lower edge). Unlike those lesions with IB margins, those with IC margins grow, infiltrating the marrow space at a rate that exceeds destruction of the adjacent trabecular bone. Trabecular destruction occurs over a wide zone *(arrows)* and is perceived radiographically as an ill-defined margin. (AFIP Neg. Nos. 69-11339-1,2, 3, 4.)

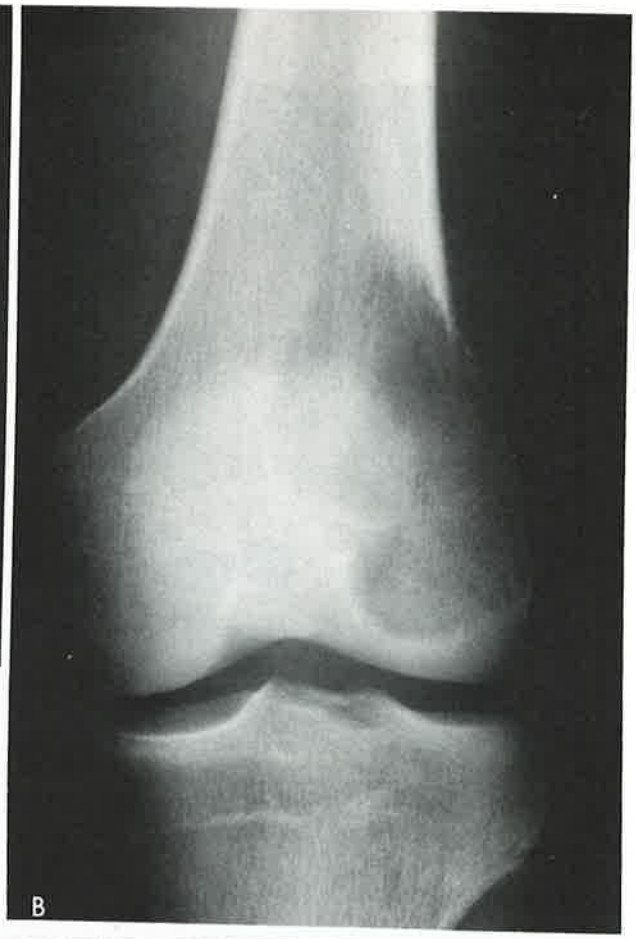

Figure 14. Type IC margins are illustrated in four cases with different diagnoses. *A,* Active enchondroma of the radius. *B,* Giant cell tumor of the femur.

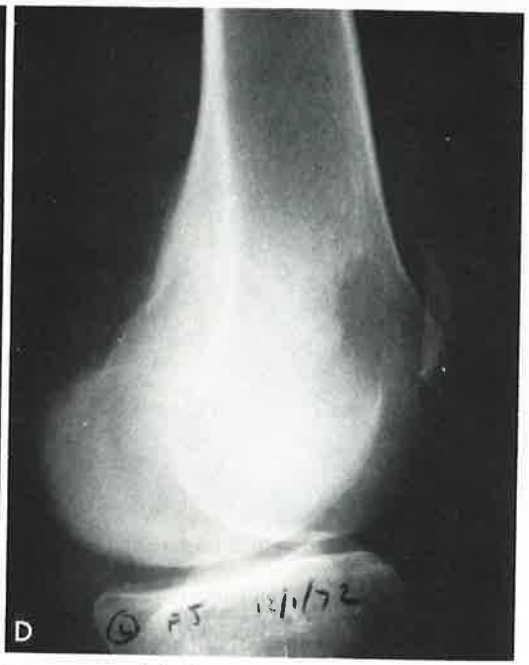

Figure 14 Continued. *C,* Chondrosarcoma of the femur. *D,* Osteosarcoma of the femur. A widened bone contour (shell) that is consistent with slow growth is seen in the enchondroma *(A),* giant cell tumor *(B),* and chondrosarcoma *(C).* Stippled areas of calcification *(A)* suggest a cartilage tumor. The margins of these lesions are ill defined (IC margins) suggesting active growth. Histologically, the enchondroma *(A)* was cellular and proliferative in appearance, but not overtly malignant, hence, the term active enchondroma. The osteosarcoma *(D)* also shows homogeneous increased marrow density that is consistent with osteoid tumor matrix calcification. (AFIP Neg. Nos. 66-13390-1, 64-4301-6, 71-10262-7, 74-5168-2.)

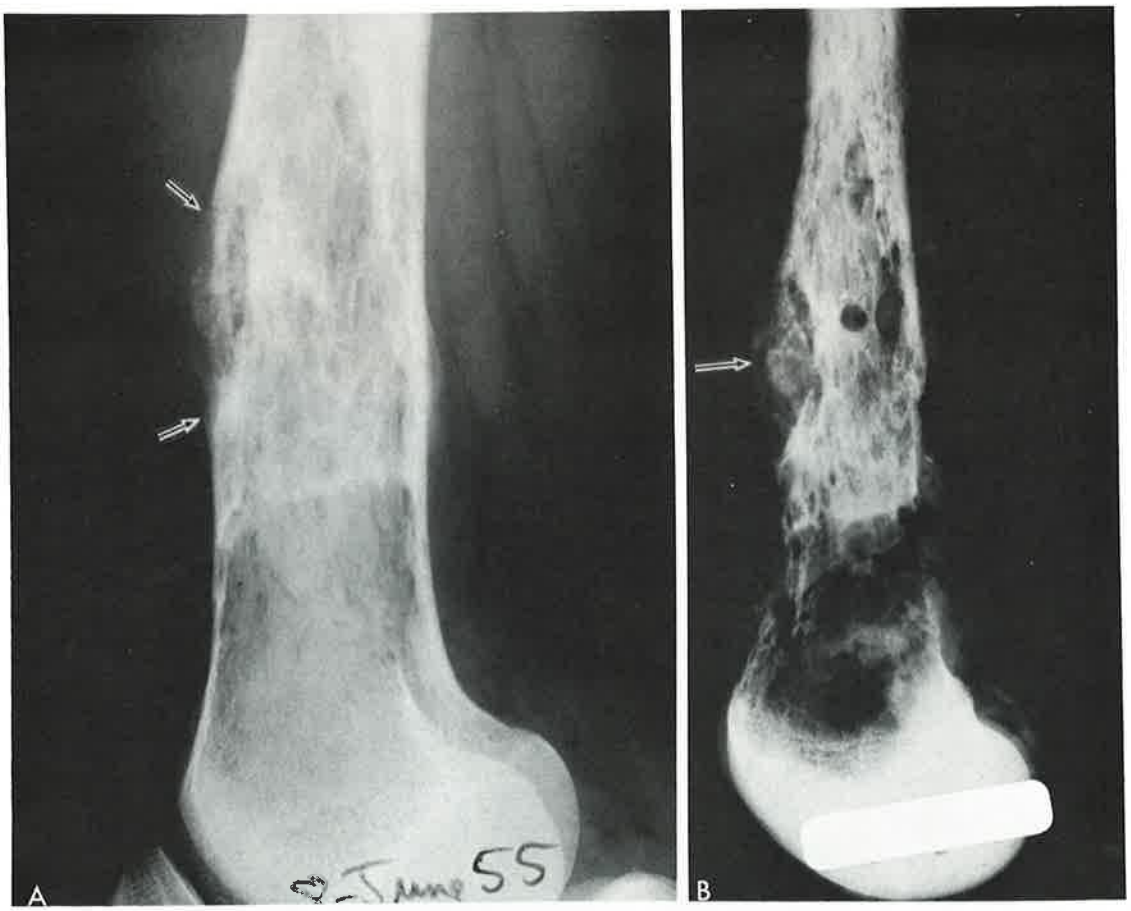

Figure 15. Type II pattern (moth-eaten), Cortical type. Osteosarcoma of the femur. *A,* A lateral view of the distal femur reveals multiple lucent holes of varying size, predominantly in the diaphysis. Focal cortical destruction with anterior breakout has created a soft tissue mass *(arrows).* An interrupted periosteal reaction borders the anterior breakout. A homogeneous increase in density (cloudy area) within the soft tissue extension is consistent with mineralization of the osteoid matrix and suggests osteosarcoma. A smaller area of posterior extension and periosteal reaction is also shown. *B,* The specimen radiograph shows, in greater detail, the moth-eaten pattern of cortical destruction in the diaphysis and the anterior breakout with sarcomatous bone *(arrow).* Two sharply circumscribed, circular, lucent biopsy sites are present in the mid portion of the shaft. Individual moth-eaten holes tend to be oval rather than circular. The tunneled pattern of proximal cortical destruction *(top)* is a product of the permeative component of this lesion.

Illustration continued on following page

15) bone, or both, may be involved. In cancellous bone, normal trabecular markings can be seen between the holes; these represent retention of cancellous bone in parts of a regionally infiltrative process (Fig. 16*D*). Occasionally, these trabecular markings may be thickened as a result of apposition of repair or tumor osteoid. Bone destruction with this pattern may be difficult to visualize early, especially if there is already a paucity of cancellous bone, as in elderly patients.

In cortical bone, deep, focal, destructive holes creating this type of pattern usually begin on the endosteal surface and erode outward (Figs. 15, *C* and *D*). This process may progress to complete destruction of the cortex and extension of the process into adjacent soft tissue. The defects are usually oval and filled by tumor (Fig. 15*D*) or inflammatory tissue (when due to infection) (Fig. 17*C*) and are lined by osteoclasts, if active. Their oval shape with the long dimension aligned parallel to the shaft is probably determined biophysically in accord with longitudinal force transmission. The result is partial retention of bone circumference with predominant bone erosion along the long axis. The moth-eaten pattern is frequently seen with malignant neoplasms (Fig. 18), such as reticulum cell sarcoma (Fig 18, *A* and *B*), osteosarcoma, chondrosarcoma (Fig. 18, *C* and *D*), fibrosarcoma, round cell tumors including Ewing sarcoma (Fig. 18*E*), and also osteomyelitis (Fig. 17).

Text continued on page 739

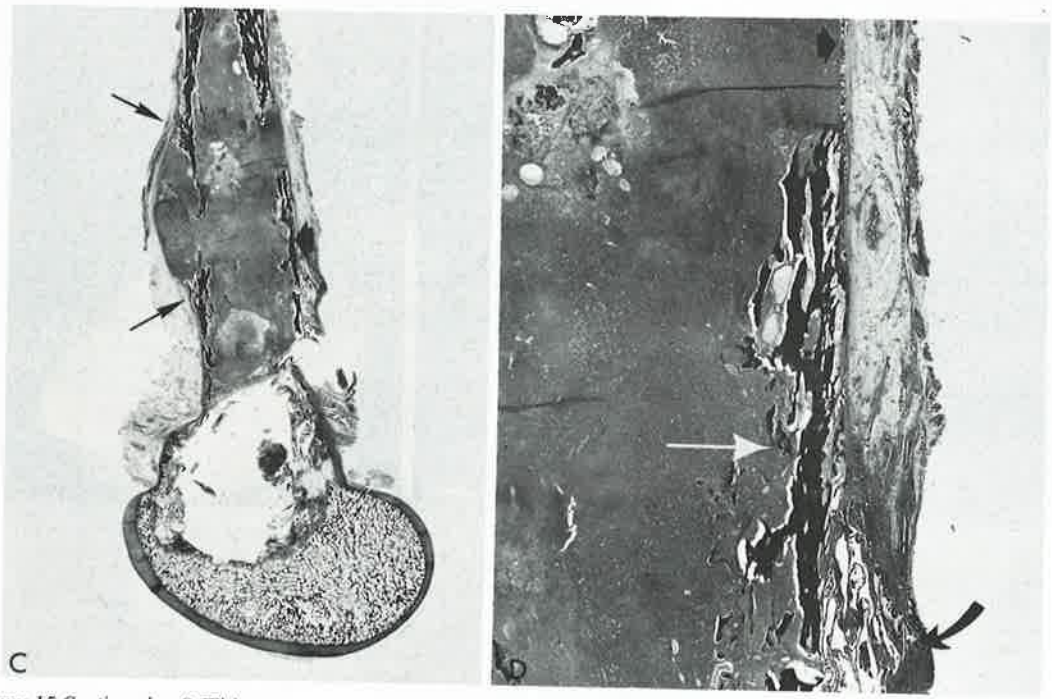

Figure 15 Continued. *C,* This macrosection (magnification × ¾) demonstrates extensive marrow-filling and shows the cystic metaphyseal component of the osteosarcoma. Histologic details of the anterior breakout *(between the arrows)* and an interrupted periosteal reaction at the edges *(arrows)* correlate well with the radiographs. The cortex beneath the anterior soft tissue breakout has been destroyed. Many sites of endosteal destruction *(arrowhead)* correspond to the multiple lucent holes of the cortical type (moth-eaten pattern). *D,* A photomicrograph (magnification × 3.2) of the posterior cortical margin (*C,* arrowhead area) displays the stages of cortical destruction responsible for this cortical type of moth-eaten pattern. First, there is focal endosteal resorption *(white arrow),* followed by complete cortical destruction *(arrowhead)* and eventual subperiosteal and soft tissue extension *(curved arrow).* Thus, the moth-eaten pattern in the diaphysis is attributable to multiple destructive foci with tumor extending through the cortex into the adjacent soft tissue. (AFIP Neg. Nos. 56-13062, 56-13063, 56-13062-1, 2.)

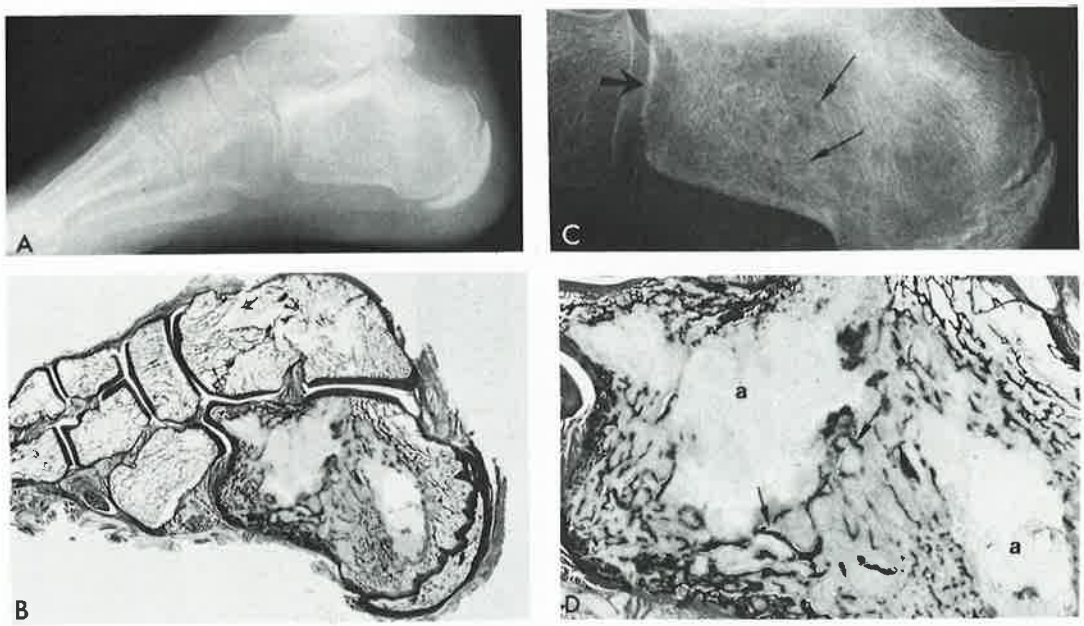

Figure 16. Type II pattern (moth-eaten), cancellous type. Fibrosarcoma of the calcaneus bone. *A,* A clinical radiograph in the lateral position demonstrates multiple lucent holes of varying sizes that involve the major portion of the calcaneus bone. There are focal areas of cortical destruction in the anterior calcaneus bone and osteoporosis in the tarsal bones, especially in the cuboid. *B,* A macrosection (magnification × 9/10) confirms the destructive pattern and distribution of the tumor. *C,* A coned-down view of the calcaneus bone in a lateral position more clearly demonstrates the multiple lucent holes of varying size *(arrows)* that are scattered throughout the calcaneous bone, as well as the anterior cortical destruction *(thick arrow).* There is some sclerosis in the superior aspect of the calcaneus bone beneath the talus, and about some of the areas of moth-eaten destruction. *D,* A histologic view (magnification × 2.2) of the calcaneus bone reveals areas of complete cancellous bone destruction (a) and residual trabecular bone *(arrows)* encased by tumor. This residual trabecular bone corresponds to the indistinct margins about the moth-eaten lucencies seen on the radiograph *(C).* Residual cancellous bone around individual holes and along the superior and inferior aspect of the calcaneus bone is thickened by reparative bone applied to pre-existing trabecular units. This represents an adaptation intended to meet the mechanical requirements of the calcaneus bone in the presence of an infiltrative, growing tumor. (AFIP Neg. Nos. 56-18983, 56-18983-1, 56-18985, 56-18983-2.)

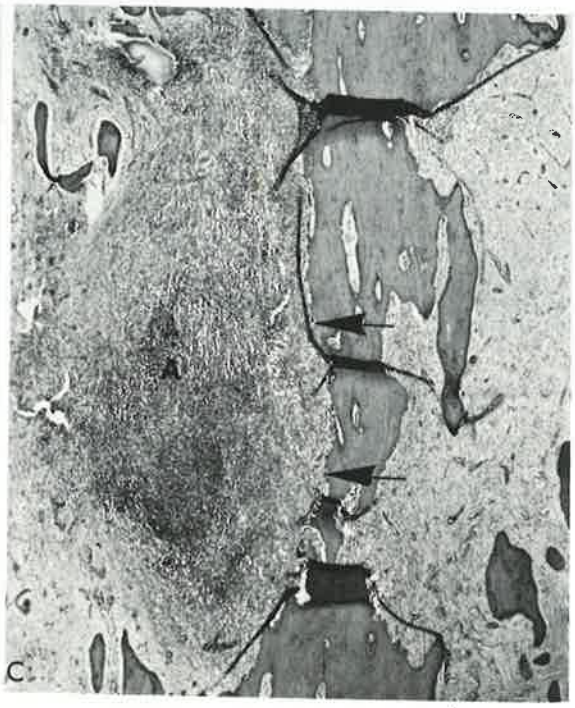

Figure 17. Type II pattern (moth-eaten), cortical type. Osteomyelitis of the tibia. *A,* Anteroposterior *(left)* and oblique *(right)* views of the tibia show diffuse, moth-eaten destruction in the diaphysis with minimal periosteal reaction. The lucent holes are predominatly focal areas of bone destruction within the cortex. *B,* Focal areas of cortical destruction arising from the endosteal *(arrows)* and periosteal *(arrowheads)* surfaces and periosteal new bone production are noted on the macrosection (magnification .4.6). *C,* A photomicrograph (magnification × 15) of an area of endosteal cortical destruction demonstrates a cortical abscess (A) with intense osteoclastic resorption *(arrows)* around its periphery. A background of granulation tissue is also present. (AFIP Neg. Nos. 292714-1, 3, 81-13771.)

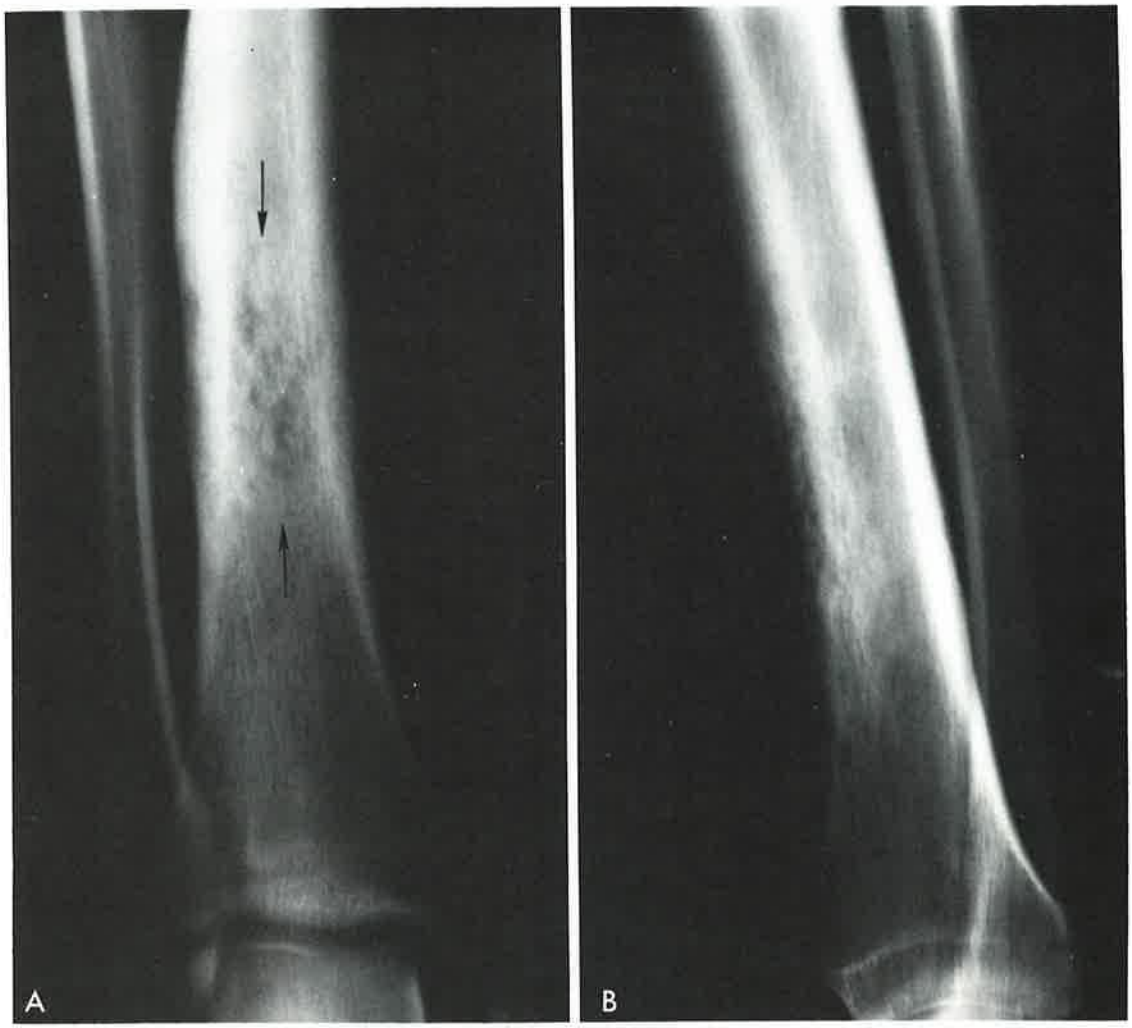

Figure 18. Type II patterns (moth-eaten) are demonstrated in multiple cases with different diagnoses. *A* and *B*, Reticulum cell sarcoma of the tibia. Anteroposterior and lateral tomograms of the tibia show moth-eaten destruction of the cortical type. Lucent holes in the cortex with a minimal periosteal reaction are superimposed over the marrow space on the anteroposterior view *(between the arrows). B,* A lateral radiograph demonstrates the lucencies as being predominantly in the anterior cortex. Marrow involvement confirmed at surgery is not detectable in these radiographs other than as reflected in the moth-eaten cortex.

Illustration continued on following page

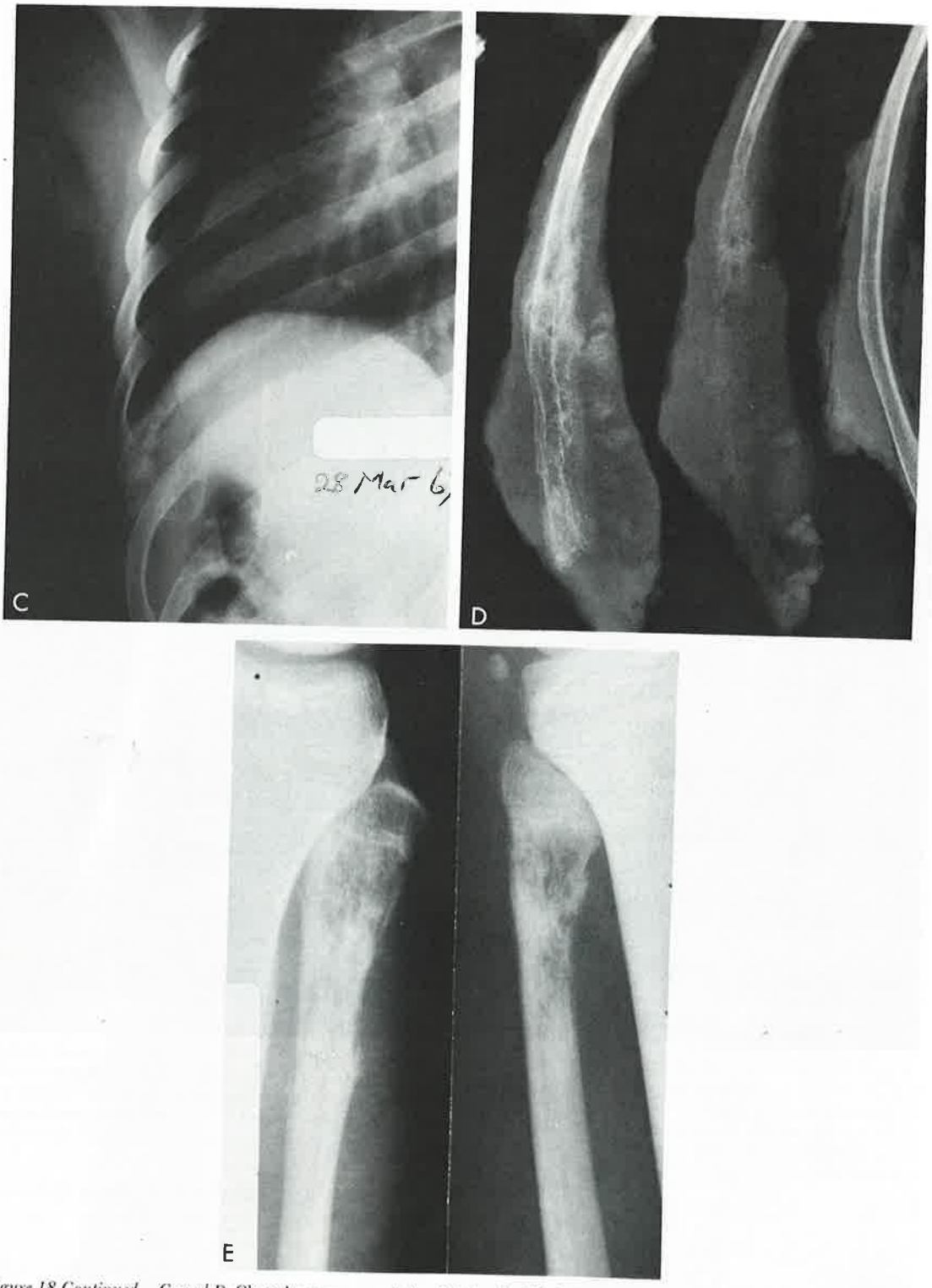

Figure 18 Continued. *C, and D,* Chondrosarcoma of the eighth rib. Clinical (*C*) and specimen (*D*) radiographs show a regionally infiltrating tumor with moth-eaten cortical destruction and a partially mineralized extension into the adjacent soft tissue. *E,* Round cell sarcoma of the fibula. Composite anteroposterior (*left*) and lateral (*right*) views show moth-eaten destruction of both metaphyseal trabecular bone and diaphyseal cortical bone. Codman angles are visible at the inferior aspects. (AFIP Neg. Nos. 72-18020-6,2, 67-5091-1,2, 56-9614-1,2.)

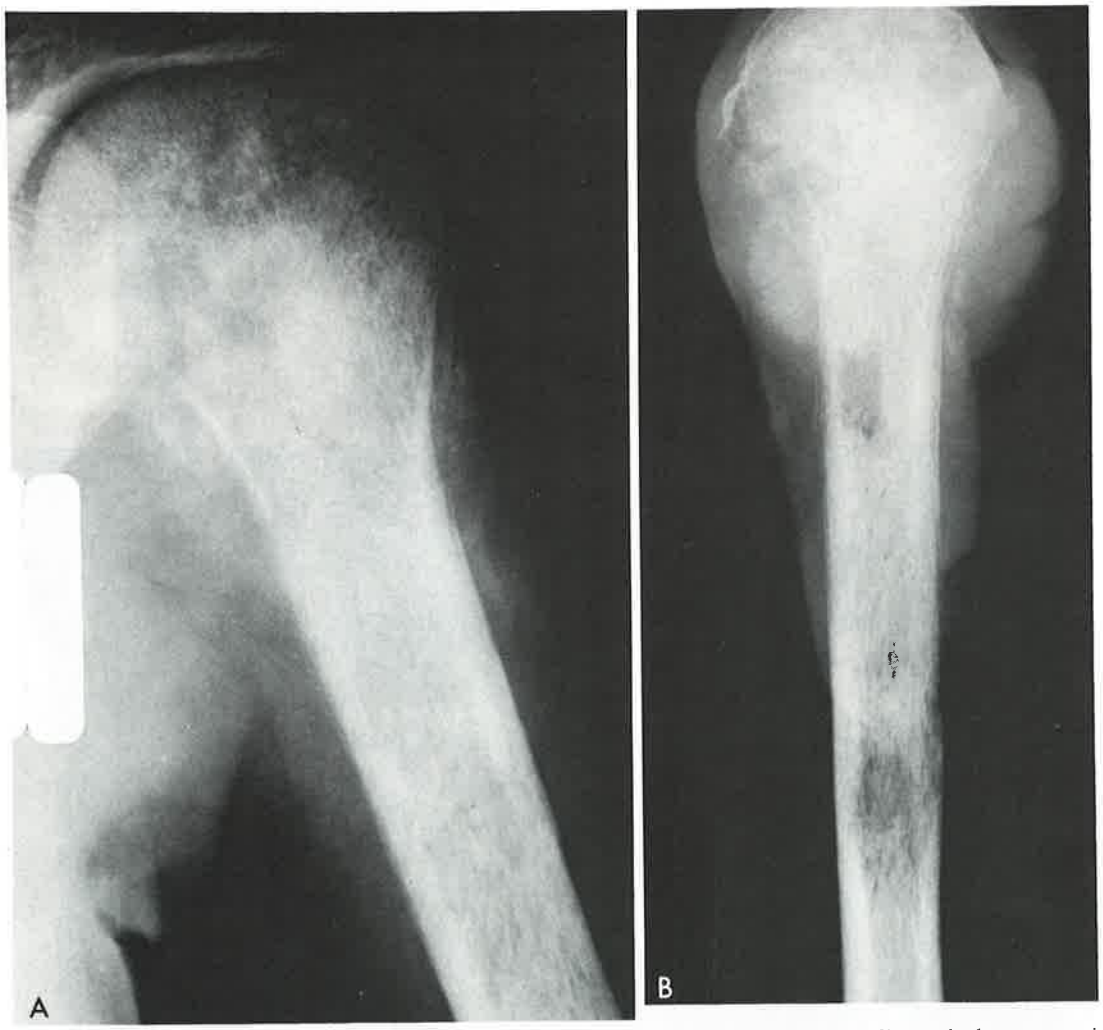

Figure 19. Type III pattern (permeative). Osteosarcoma of the humerus. *A,* A clinical radiograph shows extensive bone destruction, multiple cortical lucencies, "sunburst" soft tissue extension from the metaphysis, and periosteal reaction. *B,* A specimen radiograph confirms extensive destruction throughout the proximal humerus and extension into soft tissue. The long axes of the multiple linear oval radiolucencies are parallel to the shaft. A rectangular radiolucency located on the medial aspect is a biopsy site.

Illustration continued on following page

Permeative Destruction (Type III)

Permeative destruction in cortical bone appears as multiple, uniformly tiny, oval lucencies or lucent streaks. These are created by cortical tunneling by osteoclastic cutting cones in an accelerated caricature of the resorption phase of normal haversian remodeling (Figs. 19, *C* and *D*, and 20, *C* and *D*). It may be seen in several disease categories, including neoplastic (Fig. 21*A*), mechanical (Fig. 21*D*), inflammatory (Fig. 21*E*), and metabolic (Figs. 20 and 21, *B* and *C*). In all of these, progressive cortical lucency occurs when there is exuberant tunneling by osteoclastic cutting cones. These may or may not be accompanied by tumor or inflammatory infiltrates and, in large part, represent vascular adjustment. Coned-down views and specimen radiographs look similar regardless of the inciting process. Associated malignant lesions tend to be those that infiltrate the marrow space diffusely, for example, primary round cell sarcomas including Ewing's sarcoma and reticulum cell sarcoma. Fibrosarcoma, high grade chondrosarcoma, and angiosarcoma may also be aggressive enough to do so.

Text continued on page 744

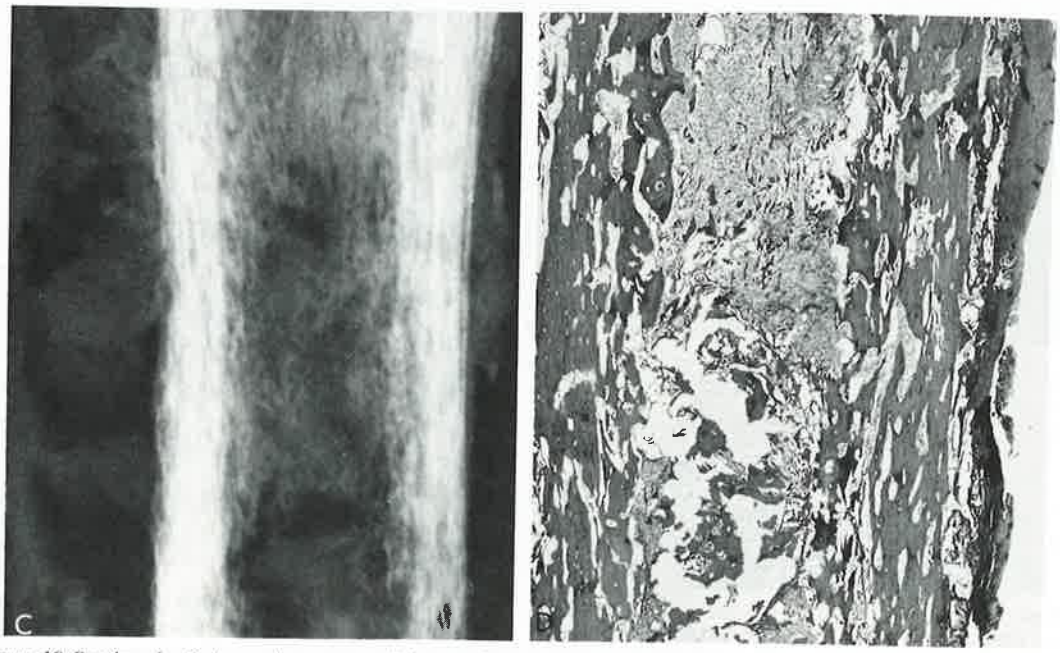

Figure 19 Continued. *C*, An enlargement of the specimen radiograph further delineates the linear destructive cortical foci, *D*, A macrosection (magnification × 2.5) shows the oval cortical radiolucencies to be cortical resorptive units similar to cutting cones of remodeling; some are involved with tumor and some are not. The tumor has filled the marrow space and broken out into the subperiosteal region. This permeative pattern is one of the more aggressive destructive radiographic patterns and is frequently associated with malignant lesions such as osteosarcoma, chondrosarcoma, and Ewing's sarcoma. (AFIP Neg. Nos. 59-7026-3, 1, 4, 5.)

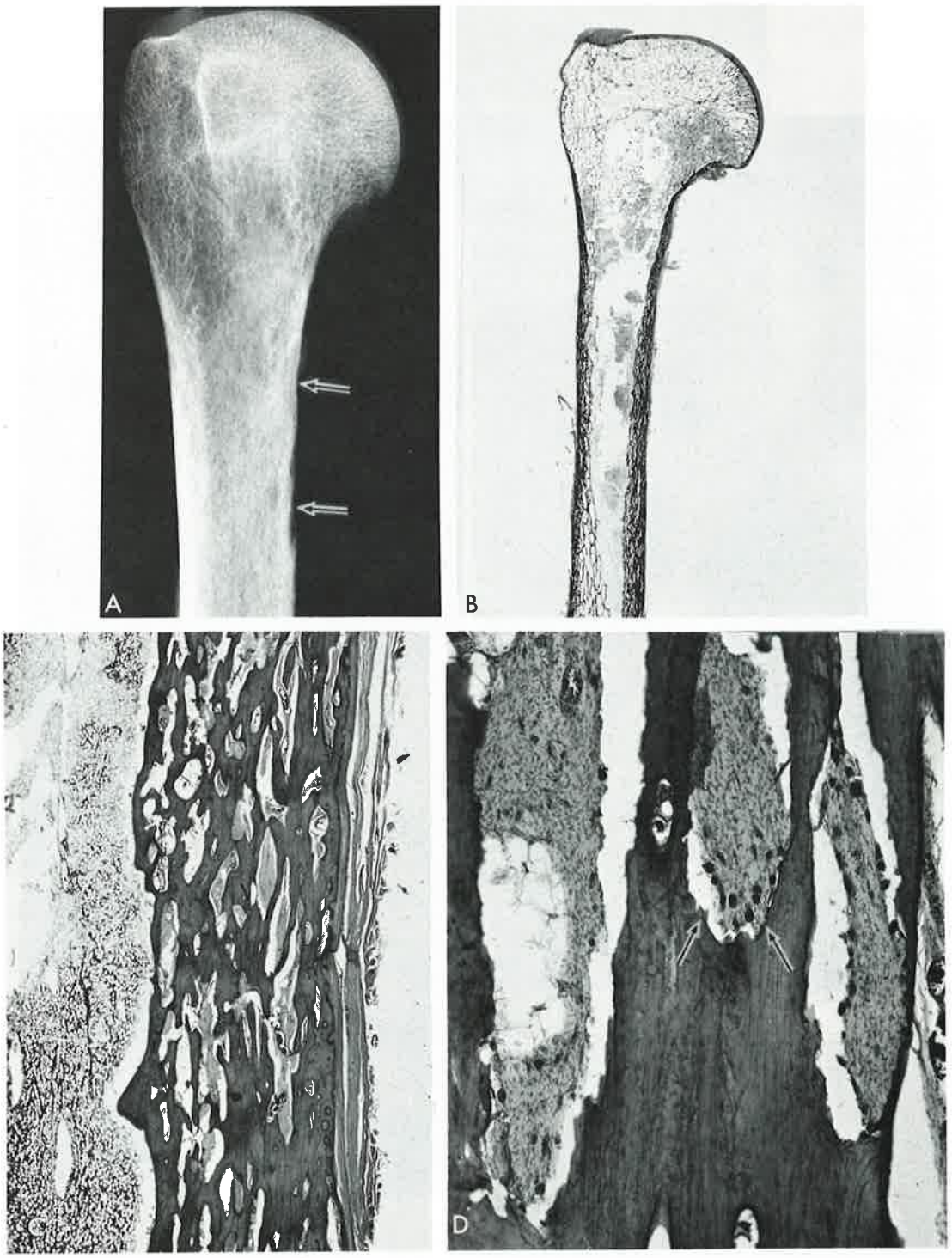

Figure 20. Type III pattern (permeative). Hyperparathyroidism affecting the humerus. *A,* A specimen radiograph demonstrates diffuse permeative destruction throughout the humeral cortex with focal subperiosteal resorption along the proximal medial aspect *(arrows).* The cortical lucencies are fairly uniform in size, with their long axes parallel to the cortex. *B,* A macrosection (magnification × 3/4) shows the diffuse, linear, cortical lucencies seen on the radiograph. *C,* A power view of the humeral cortex (magnification × 13) demonstrates the oval, focal, resorbed areas that are filled with fibrovascular tissue. The marrow is normal. *D,* A photomicrograph (magnification × 63) confirms the elongated cortical oval lucencies that are present as a result of accelerated osteonal remodeling (cutting cone or tunneling) of the cortex. Teams of osteoclastic cells are the vanguard of the advancing destructive front *(arrows)* of each resorptive unit. Accelerated cortical remodeling (tunneling) is the mechanism of permeative bone destruction, whether it is seen in metabolic (hyperparathyroidism, active osteoporosis), mechanical, inflammatory, or neoplastic disease states. (AFIP Neg. Nos. 59-6666-3, 81,13772-2,4, 81-3780-1.)

Figure 21. Type III patterns (permeative) are demonstrated in multiple cases with different diagnoses. All of these cases have the characteristic permeative, cortical, destructive pattern that is secondary to exaggerated internal remodeling. The specific diagnoses in these cases are not made by the cortical destructive pattern, but can be predicted from anatomic location of the lesion, associated clinical findings, and other radiographic features. Examples of this comprehensive analytic approach include: Ewing's sarcoma (*A*), which is accompanied by permeative destruction plus mixed spiculated and lamellated periosteal reactions; hyperparathyroidism (*B* and *C*), which is marked by diffuse, cortical tunneling of multiple bones, subperiosteal resorption, and brown tumors; a stress reaction of the ulna (*D*), which is accompanied by an oblique cortical infraction supported by an appropriate clinical history; and osteomyelitis (*E*), with which systemic signs and symptoms of sepsis may appear. (AFIP Neg. Nos. 65-2291-1, 75-3779-5, 8, 77-4546-4, 65-496-1.)

Illustration continued on opposite page

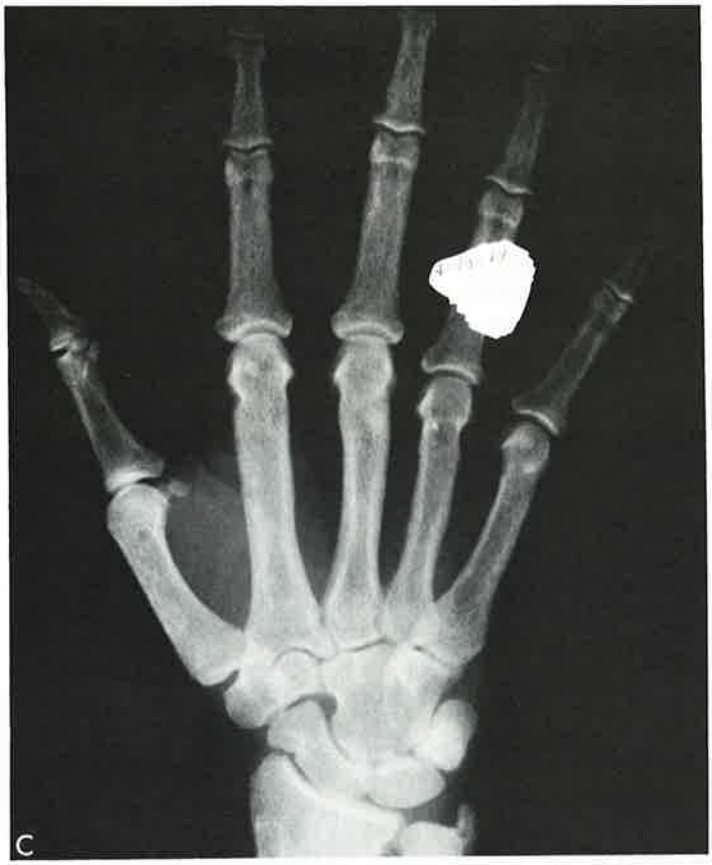

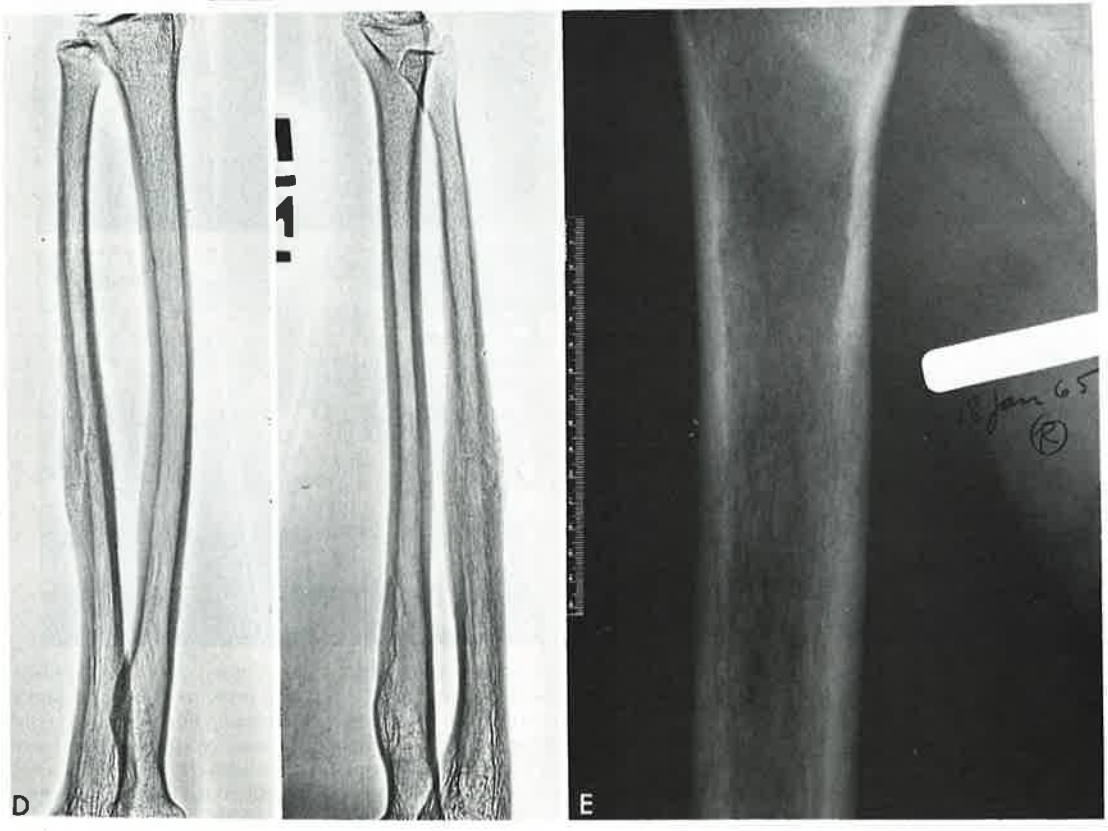

Figure 21. See legend on opposite page.

Combination and Changing Patterns

Any combination of types IA, IB, IC, II, and III margins in a single lesion constitutes a combination pattern (Fig. 22) and is suggestive of a change toward more aggressive local growth. Combination patterns may be seen when benign lesions become active, undergo malignant transformation, or fracture. Pressure from tumor growth and active hyperemia are major factors producing these changes. The distinction between a combination pattern (Fig. 22) and a changing margin (Fig. 23) may be made by observing a sequence of radiographs that document the change in the latter.

Before concluding this discussion of margins, it should be pointed out that the fastest rate of tumor growth through a cancellous network is signified by little or no radiographic change in density or pattern (Fig. 24). Very rapid filling of the cancellous or diaphyseal marrow space with tumor deletes, by displacement or infarction, all soft tissue elements, including osteoclasts, osteoblasts, and blood vessels. Pre-existent bone completely encased in sarcoma tends to persist with its original "normal" density and architecture (Figs. 24, *C* and *D*). This is equivalent to an "invisible" tumor margin. Such a cancellous system can appear relatively more dense if reflex vascular or disuse osteoporosis, or both, reduces the density of surrounding normal bone. In this setting, tumor proliferation proceeds mainly in the better vascularized periphery, whereas the center is commonly necrotic. Invisible margins are most often associated with aggressive, matrix-producing sarcomas in which unmineralized cartilage predominates (Fig. 24).

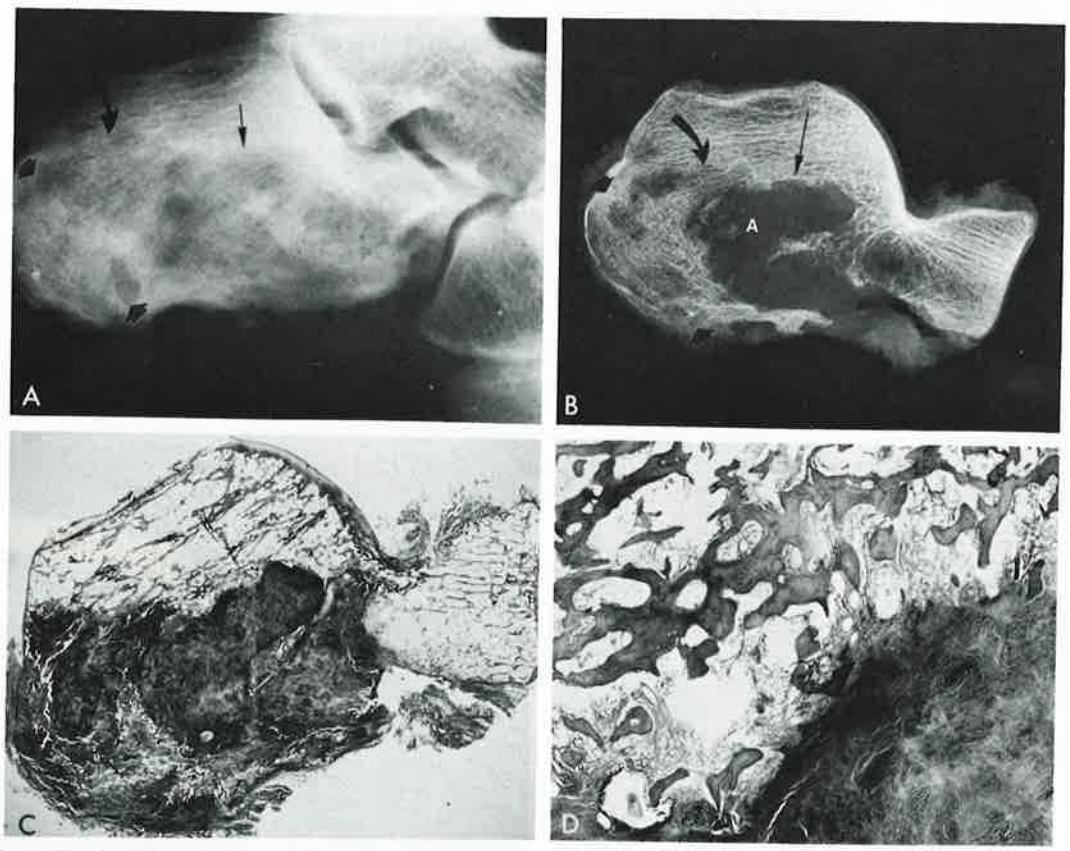

Figure 22. Combined pattern. Fibrosarcoma of the calcaneus bone. Clinical *(A)* and specimen *(B)* radiographs in a lateral position demonstrate a diffuse destructive process of the calcaneus bone. Geographic margins of types IA and IB *(straight arrow)*, IC *(curved arrow)*, II (regional or moth-eaten destruction) *(area between arrowheads)*, and complete central osteolysis at point "A" are apparent. *C*, A macrosection (magnification × 1.5) confirms the overall geographic distribution of this process; a well-defined superior margin and a regionally infiltrating margin *(left)* are seen. *D*, Marginal sclerosis (type IA), which is best demonstrated radiographically in *B*, corresponds to the appositional reparative bone on pre-existing trabeculae that is shown in this photomicrograph (magnificatin × 11). (AFIP Neg. Nos. 299181-1,2,4,5.)

Figure 23. Changing margin. Sarcoma arising in a bone cyst of the humerus. *A,* The clinical radiograph shows a pathologic fracture through a lucent geographic lesion. It has a mixed margin of type IA distally, a type IB margin with a shell proximally and medially, and a type IC margin proximally and superolaterally. The distal type IA margin has a very thick sclerotic rim. *B,* A radiograph taken 5½ months later documents lytic extension into the epiphysis and substantial destruction of the distal sclerotic rim. Changing margins imply accelerated biologic activity, such as aggressive malignancy arising in a slower or benign process. (AFIP Neg. Nos. 76-2618-1,2.)

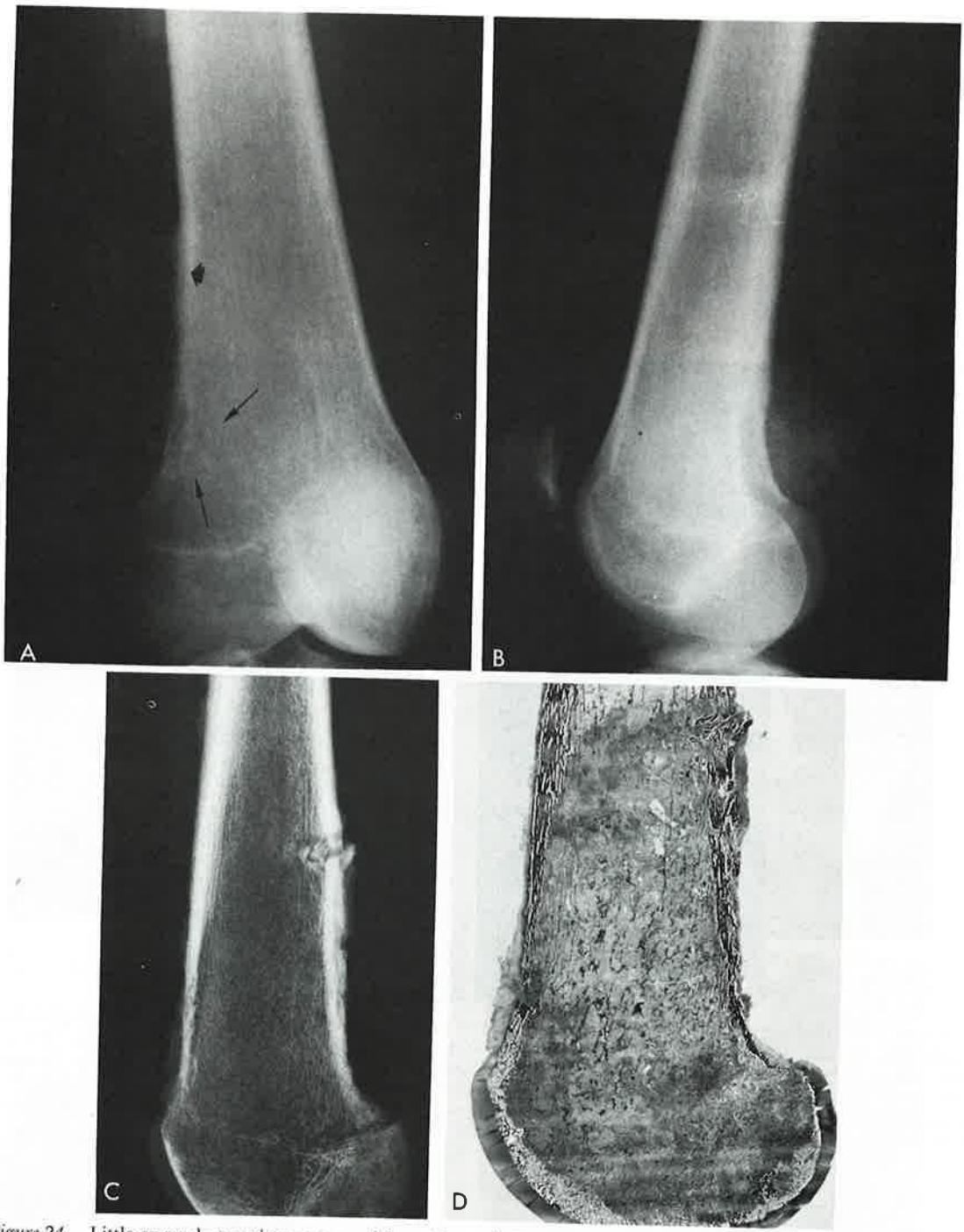

Figure 24. Little or no destruction seen on plain radiograph ("invisible margin"). Chondrosarcoma of the femur. *A* and *B,* Anteroposterior and lateral radiographs show a posterolateral soft tissue mass with mineralization, periosteal reaction *(arrowhead),* and minimal bone destruction *(arrows). C,* Small, patchy radiolucencies are seen on the specimen radiograph in the posterior distal femur. Biopsy defects penetrate the posterior cortex. Most of the cortical and trabecular patterns are intact on the specimen radiograph; however, the macrosection (magnification × 1) *(D)* comfirms that the tumor fills most of the distal femur. It also demonstrates small areas of soft tissue extension through the anterior and posterior cortex. This discrepancy can be seen in malignant lesions that grow extemely rapidly, including sarcomas (chondrosarcoma, osteosarcoma, Ewing's sarcoma) and lymphomas, as well as acute osteomyelitis.

Illustration continued on opposite page

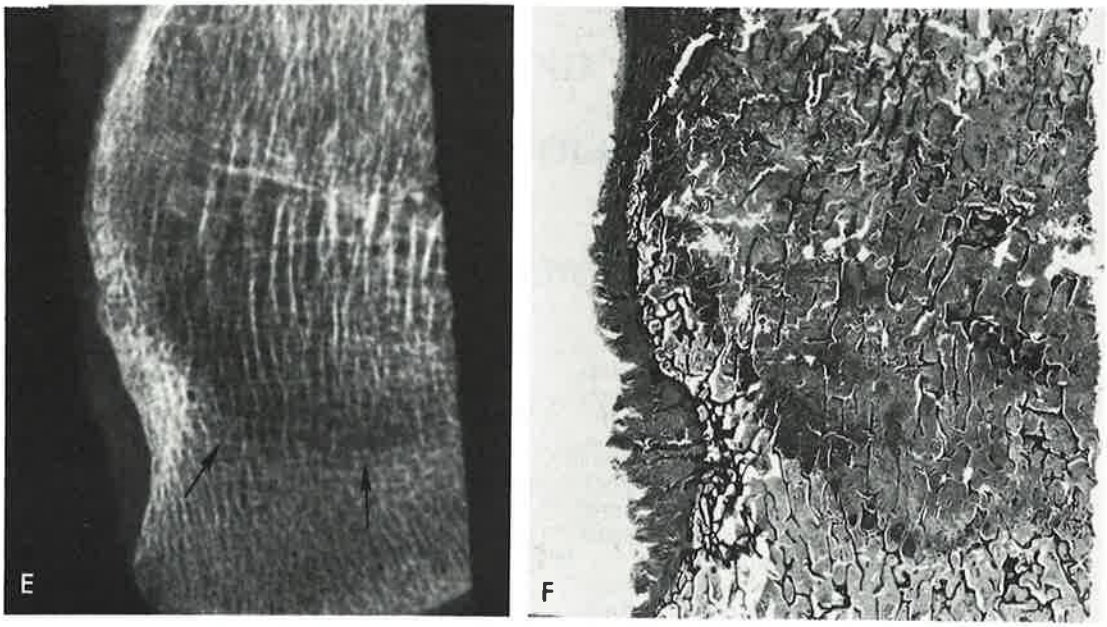

Figure 24 Continued. *E,* A coned-down view of an anteroposterior frontal specimen radiograph of the distal femur shows subtle bone lysis with an ill-defined edge (type IC) *(arrow). F,* The histologic preparation that corresponds (magnification ×3.2) to *E* confirms diffuse infiltration and solid replacement of the marrow space by tumor, with only minimal trabecular destruction. (AFIP Neg. Nos. 70-11170-3,4, 81-14575, 81-14581, 81-14576, 81-14637.)

SUMMARY

The margin or interface between tumor and bone (cortical or cancellous) that is displayed radiographically is a zone of cellular activity. Its radiographic appearance represents the summation of bone lysis (osteoclastic activity) and production (osteoblastic activity). This activity and the radiographic details of the resultant margin are an index of the biologic activity of a lesion. The anatomic site and extent of the lesion can be assessed by radiographs and special imaging techniques. Careful analysis of these patterns, when integrated with clinical data, enhances diagnosis, patient management, and therapy.

ACKNOWLEDGMENT

We thank the many contributing radiologists and pathologists whose case material illustrated this work, as well as the Armed Forces Institute of Pathology's secretarial and technical staff of the Departments of Radiologic Pathology, Orthopedic Pathology, and Medical Illustration, for their assistance.

REFERENCES

1. Ardran, G. M.: Bone destruction not demonstrable by radiography. Brit. J. Radiol., *24*:107–109, 1951.
2. Arnold, J. S.: The quantitation of bone mineralization as an organ and tissue in osteoporosis. *In* Pearson, O. H., and Joplin, G. F. (eds.): Dynamic Studies of Metabolic Bone Disease. Oxford, Blackwell Scientific Publishers, 1964, pp. 59–76.
3. Belanger, L. F., and Migicovsky, B. B.: Histochemical evidence of proteolysis in bone; the influence of parathormone. J. Histochem. Cytochem., *11*:734–737, 1963.
4. Bloom, W. F., and Faucett, D. W.: Bone. *In* A Textbook of Histology. Ch. 7. Philadelphia, W. B. Saunders Company, 1962, p. 164.
5. Codman, E. A.: Epiphyseal chondromatous giant cell tumors of the upper end of the humerus. Surg. Gynecol. Obstet., *52*:543–548, 1931.
6. Codman, E. A.: The nomenclature used by the registry of bone sarcoma. Am. J. Roentgenol. *13*:105–126, 1925.
7. Codman, E. A.: Registry of bone sarcoma. Surg. Gynecol. Obstet., *42*:381–393, 1926.
8. Codman, E. A.: The registry of cases of bone sarcoma. Surg. Gynecol. Obstet., *34*:335–343, 1922.
9. Codman, E. A.: Treatment of giant cell tumors about the knee. Study of 153 cases collected by Registry of Bone Sarcoma of the American College of Surgeons. Surg. Gynecol. Obstet., *64*:485–496, 1937.

10. Edeiken, J., and Hodes, P. J.: Basic considerations of bone and cartilage. *In* Roentgen Diagnosis of Diseases of Bone. Ed. 2. Ch. 1. Baltimore, Williams and Wilkins Company, 1973.
11. Edeiken, J., and Hodes, P. J.: General radiologic approach to bone lesions. *In* Roentgen Diagnosis of Diseases of Bone. Ed. 2. Ch. 3. Baltimore, Williams and Wilkins Company, 1973.
12. Ewing, J.: A review and classification of bone sarcomas. Arch. Surg., *4*:485–533, 1922.
13. Genant, H. K., Kozin, F., Bekerman, C., et al.: The reflex sympathetic dystrophy syndrome. Radiology, *117*:21–32, 1975.
14. Hancock, N. M., and Boothroyd, B.: Structure-function relationships in the osteoclast. *In* Mechanism of Hard Tissue Destruction. Ch. 18. Washington, D.C., American Association for the Advancement of Science, 1963, pp. 497–514.
15. Johnson, L. C.: A general theory of bone tumors. Bull. N.Y. Acad. Med., *29*:164–171, 1953.
16. Johnson, L. C.: The kinetics of skeletal remodeling. *In* Structural Organization of the Skeleton. Birth Defect Original Article Series, Vol. 2. National Foundation, March of Dimes, April, 1966.
17. Johnson, L. C.: Morphologic analysis in pathology. The kinetics of disease and general biology of bone. *In* Frost, H. M. (ed.): Bone Biodynamics. Ch. 29. Boston, Little, Brown and Company, 1964, pp. 543–654.
18. Lachman, E.: Osteoporosis: The potentialities and limitations of its roentgenologic diagnosis. Am. J. Roentgenol., *74*:712–715, 1955.
19. Lodwick, G. S.: The bone and joints. *In* Atlas of Tumor Radiology. Chicago Yearbook Medical Publishers Inc., 1971.
20. Lodwick, G. S.: Radiographic diagnosis and grading of bone tumors with comments on computer evaluation. *In* Proceedings of the Fifth National Cancer Conference. Philadelphia, Sept. 17–19, 1964, pp. 369–380.
21. Lodwick, G. S.: Reactive response to local injury in bone. RADIOL. CLIN. NORTH AM., *2*:209–219, 1964.
22. Lodwick, G. S.: A systemic approach to the roentgen diagnosis of bone tumors. *In* M. D. Anderson Hospital and Tumor Institute: Tumors of Bone and Soft Tissue. Chicago, Yearbook Medical Publishers Inc., 1965, pp. 49–68.
23. Lodwick, G. S., Wilson, A. J., Farrell, C., et al.: Determining growth rates of focal lesions of bone from radiographs. Radiology, *134*:577–583, 1980.
24. McLean, F. C., and Urist, M. R.: Bone Fundamentals of Physiology of Skeletal Tissue. Ed. 3. Chicago, The University of Chicago Press, 1968.
25. Meema, H. E., and Schatz, D. L.: Simple radiographic demonstration of cortical bone loss in thyrotoxicosis. Radiology, *97*:9–15, 1970.
26. Meema, H. E., Oreopoulos, D. G., and Meema, S.: A roentgenologic study of cortical bone resorption in chronic renal failure. Radiology, *126*:67–74, 1978.
27. Parker, F., and Jackson, H.: Primary reticulum cell sarcoma of bone. Surg. Gynecol. Obstet., *68*:45–53, 1939.
28. Phemister, D. B.: A study of the ossification in bone sarcoma. Radiology, *7*:17–23, 1926.
29. Schinz, H. R., Baensch, W. E., Friedl, E., et al.: Skeleton. Part 1. *In* Roentgen Diagnostics. American Ed. 1. (Translated by J. T. Case.) Vol. 1. New York, Grune and Stratton, 1951, p. 110.
30. Steiner, G. C., Ghosh, L., and Dorfman, H. D.: Ultrastructure of giant cell tumors of bone. Human Pathol., *3*:569–586, 1972.
31. Weiss, C.: Normal roentgen variant: Cortical tunneling of the distal ulna. Radiology, *136*:294, 1980.
32. Weiss, P.: Deformities as cues to understanding development of form. Perspect. Biol. Med., *4*:133–151, 1961.
33. Wolff, J.: Das Gesetz der Transformation der Knochen. Berlin, A. Hirschwold, 1892.

Department of Radiologic Pathology
Armed Forces Institute of Pathology
Washington, D.C. 20306